ORIGINAL RESEARCH

Mitochondrial Aldehyde Dehydrogenase 2 Plays Protective Roles in Heart Failure After Myocardial Infarction via Suppression of the Cytosolic JNK/p53 Pathway in Mice

Aijun Sun, PhD;* Yunzeng Zou, MD, PhD;* Ping Wang, PhD;* Danling Xu, PhD;* Hui Gong, PhD;* Shijun Wang, PhD; Yingjie Qin, PhD; Peng Zhang, MD; Yunqin Chen, MD; Mutsuo Harada, PhD; Toyoshi Isse, PhD; Toshihiro Kawamoto, PhD; Huizhi Fan, PhD; Pengyuan Yang, PhD; Hiroshi Akazawa, PhD; Toshio Nagai, MD; Hiroyuki Takano, MD; Peipei Ping, PhD; Issei Komuro, MD, PhD; Junbo Ge, MD

***Background*—**Increasing evidence suggests a critical role for mitochondrial aldehyde dehydrogenase 2 (ALDH2) in protection against cardiac injuries; however, the downstream cytosolic actions of this enzyme are largely undefined.

***Methods and Results*—**Proteomic analysis identified a significant downregulation of mitochondrial ALDH2 in the heart of a rat heart failure model after myocardial infarction. The mechanistic insights underlying ALDH2 action were elucidated using murine models overexpressing ALDH2 or its mutant or with the ablation of the *ALDH2* gene (*ALDH2* knockout) and neonatal cardiomyocytes undergoing altered expression and activity of ALDH2. Left ventricle dilation and dysfunction and cardiomyocyte death after myocardial infarction were exacerbated in *ALDH2*-knockout or ALDH2 mutant-overexpressing mice but were significantly attenuated in ALDH2-overexpressing mice. Using an anoxia model of cardiomyocytes with deficiency in ALDH2 activities, we observed prominent cardiomyocyte apoptosis and increased accumulation of the reactive aldehyde 4-hydroxy-2-nonenal (4-HNE). We subsequently examined the impacts of mitochondrial ALDH2 and 4-HNE on the relevant cytosolic protective pathways. Our data documented 4-HNE-stimulated p53 upregulation via the phosphorylation of JNK, accompanying increased cardiomyocyte apoptosis that was attenuated by inhibition of p53. Importantly, elevation of 4-HNE also triggered a reduction of the cytosolic HSP70, further corroborating cytosolic action of the 4-HNE instigated by downregulation of mitochondrial ALDH2.

***Conclusions*—**Downregulation of ALDH2 in the mitochondria induced an elevation of 4-HNE, leading to cardiomyocyte apoptosis by subsequent inhibition of HSP70, phosphorylation of JNK, and activation of p53. This chain of molecular events took place in both the mitochondria and the cytosol, contributing to the mechanism underlying heart failure. **(*J Am Heart Assoc*. 2014;3:e000779 doi: 10.1161/JAHA.113.000779)**

Key Words: ALDH2 • apoptosis • heart failure • myocardial infarction • p53

Heart failure (HF), the end-stage of various heart diseases, is a leading cause of mortality in many countries.[1] The underlying mechanisms responsible for the development of HF have not been fully understood, and thus the treatment for HF has yet to improve. HF is a complex syndrome characterized by mechanical dysfunction of the myocardium, defects in bioenergetics, increased cardiac pre- and/or after-load, maladjusted myocardial angiogenesis, altered signal transduction pathways, and abnormal calcium homeostasis; in addition, neurohormonal and inflammatory

From the Shanghai Institute of Cardiovascular Diseases, Zhongshan Hospital and Institutes of Biomedical Sciences (A.S., Y.Z., D.X., H.G., S.W., P.Z., Y.C., J.G.) and Department of Chemistry and Proteome Research Center, Institutes of Biomedical Sciences (H.F., P.Y.), Fudan University, Shanghai, China; Department of Cardiovascular Science and Medicine, Chiba University Graduate School of Medicine, Chiba, Japan (P.W., Y.Q., M.H., T.N., H.T.); Department of Environmental Health, School of Medicine, University of Occupational and Environmental Health, Fukuoka, Japan (T.I., T.K.); Department of Cardiovascular Medicine, University of Tokyo Graduate School of Medicine, Tokyo, Japan (H.A., I.K.); Division of Cardiology, Departments of Physiology and Medicine, David Geffen School of Medicine at UCLA, Los Angeles, CA (P.P.).

*Dr Sun, Dr Zou, Dr Wang, Dr Xu, and Dr Gong contributed equally to this work.

Correspondence to: Junbo Ge, MD, Yunzeng Zou, MD, PhD, or Aijun Sun, PhD, Shanghai Institute of Cardiovascular Diseases, Zhongshan Hospital, Fudan University, 180 Feng Lin Road, Shanghai 200032, China. E-mails: jbge@zs-hospital.sh.cn, zou.yunzeng@zs-hospital.sh.cn, sun.aijun@zs-hospital.sh.cn; Issei Komuro, MD, PhD, Department of Cardiovascular Medicine, University of Tokyo Graduate School of Medicine, Tokyo 113-8655, Japan. E-mail: komuro_tky2000@yahoo.co.jp

Received May 5, 2014; accepted July 11, 2014.

disorders might contribute to all of the pathogenic mechanisms of HF.[2] Moreover, the "mismatch" between the increasing energy demand of cardiomyocytes and the proliferation of mitochondria in cases of cardiac hypertrophy might promote HF development.[3,4] A majority of intracellular reactive oxygen species (ROS) are byproducts of mitochondrial metabolism, and bioenergetic activity and mitochondrial dysfunctions were shown to result in the generation of excess amounts of oxidant stress[5–8] and could further enhance cardiomyocytes apoptosis, which serves as another mechanism for the aggravation of HF.[9–11]

In a separate experiment, we found that the expression levels of 9 protein spots on gels were decreased and other 6 protein spots on gels were increased in rat heart mitochondrial proteins 4 weeks after myocardial infarction (MI) compared with a sham group using 2-dimensional (2D) electrophoresis. In addition, 1 of the decreased spots was identified as aldehyde dehydrogenase 2 (ALDH2) by a mass spectrometry and database comparison (Figure 1A through 1C; Table 1). The phenomena were confirmed in rat (Figure 1D and 1E) and mouse (Figure 2A and 2B) HF models as well as in the failing human heart (Figure 2C and 2D), stimulating our interest in exploring the role of ALDH2 in the development of HF. ALDH2 was reported to serve as a nitrate reductase that specifically catalyzes nitroglycerin and produces nitric oxide.[12,13] Chronic nitrate treatment-induced inhibition of ALDH2 is one of the reasons for nitrate tolerance.[14,15] Several lines of evidence suggest that ALDH2 could act on detoxification of acetaldehyde such as 4-hydroxy 2-nonenol (4-HNE)[16] and may be a key enzyme involved in protection against various cardiac injuries such as ischemia and ethanol toxicities.[17,18]

Although the precise mechanisms of downregulation of ALDH2 during the development of HF remain unclear, it has been shown that treatment with a PKC activator upregulated ALDH2 activity and reduced infarct size, and PKC inhibition abolished ethanol-induced increases in ALDH2 activity and cardiac protection against ischemia, suggesting that PKC might be a regulator for ALDH2.[17] In addition, our recent results showed that miR-34a was highly increased, whereas ALDH2 expression was decreased after MI in mice. Overexpression of miR-34a in neonatal rat cardiomyocyte could significantly enhance apoptosis and downregulate ALDH2 expression. Luciferase reporter assay results demonstrated that ALDH2 was a direct target of miR-34a.[19] Taken together, PKC and miR-34a might be responsible for the downregulation of ALDH2.

Although ALDH2/4-HNE have been reportedly involved in protection against various cardiac injuries, the downstream molecular actions of ALDH2/4-NHE are largely undefined. It remains unknown whether the mobilization of mitochondrial ALDH2 affects events in the cytosol and whether cardiac protection results from integrated actions from both mitochondrial and cytosolic locations. Accordingly, using a murine HF model induced by MI, we explored the potential role of ALDH2 in the development of HF and tried to clarify the related molecular chain from mitochondria to cytosol.

Table 1. List of Proteins Identified by Proteomics

1. Proteins with more than 5 fold-decrease of expression in failing heart
Mitochondrial proteins
Similar to RIKEN cDNA 1700025B16 (*Rattus norvegicus*)
Aconitase 2 (*Rattus norvegicus*)
Aldehyde dehydrogenase 2, mitochondrial (*Rattus norvegicus*)
LRRGT00108 (*Rattus norvegicus*)
Electron-transfer-flavoprotein, beta polypeptide (*Rattus norvegicus*)
Hypothetical LOC361596 (*Rattus norvegicus*)
RIKEN cDNA 2900053E13 (Mouse)
Other proteins
Myosin, light polypeptide 3 (*Rattus norvegicus*)
Predicted: similar to ribosomal protein L21 (*Rattus norvegicus*)
2. Proteins with more than 5-fold increase in expression in failing heart
Mitochondrial proteins
Dihydrolipoamide S-acetyltransferase (*Rattus norvegicus*)
RIKEN cDNA 2900053E13 (Mouse)
Other proteins
Vimentin (*Rattus norvegicus*)
Tubulin, beta 5 (*Rattus norvegicus*)
Ribosomal protein L8 (*Homo sapiens*)
Protein disulfide-isomerase A6 precursor (*Rattus norvegicus*)

Methods

Animals and Gene Manipulation

Adult male Sprague–Dawley rats (200 to 250 g) and wild type (WT) C57BL/6 mice (20 to 25 g) were purchased from Shanghai Animal Administration Center. *ALDH2*-knockout (*ALDH2*-KO) mice were generated, as described previously.[20] Adenoviral vectors encoding *ALDH2* or empty vector were injected into the left ventricular (LV) cavity through the apex of the heart.[21,22] In brief, adenoviral vectors encoding *ALDH2*, dominant negative forms of *ALDH2* (*dnALDH2),* or empty vector (10^9 pfu in 100 μL medium) were injected into the LV cavity through the apex of the heart under temporary clamping of the ascending aorta and pulmonary artery for 40 seconds 2 days prior to the MI procedure.[21] Efficacy of adenoviral vector

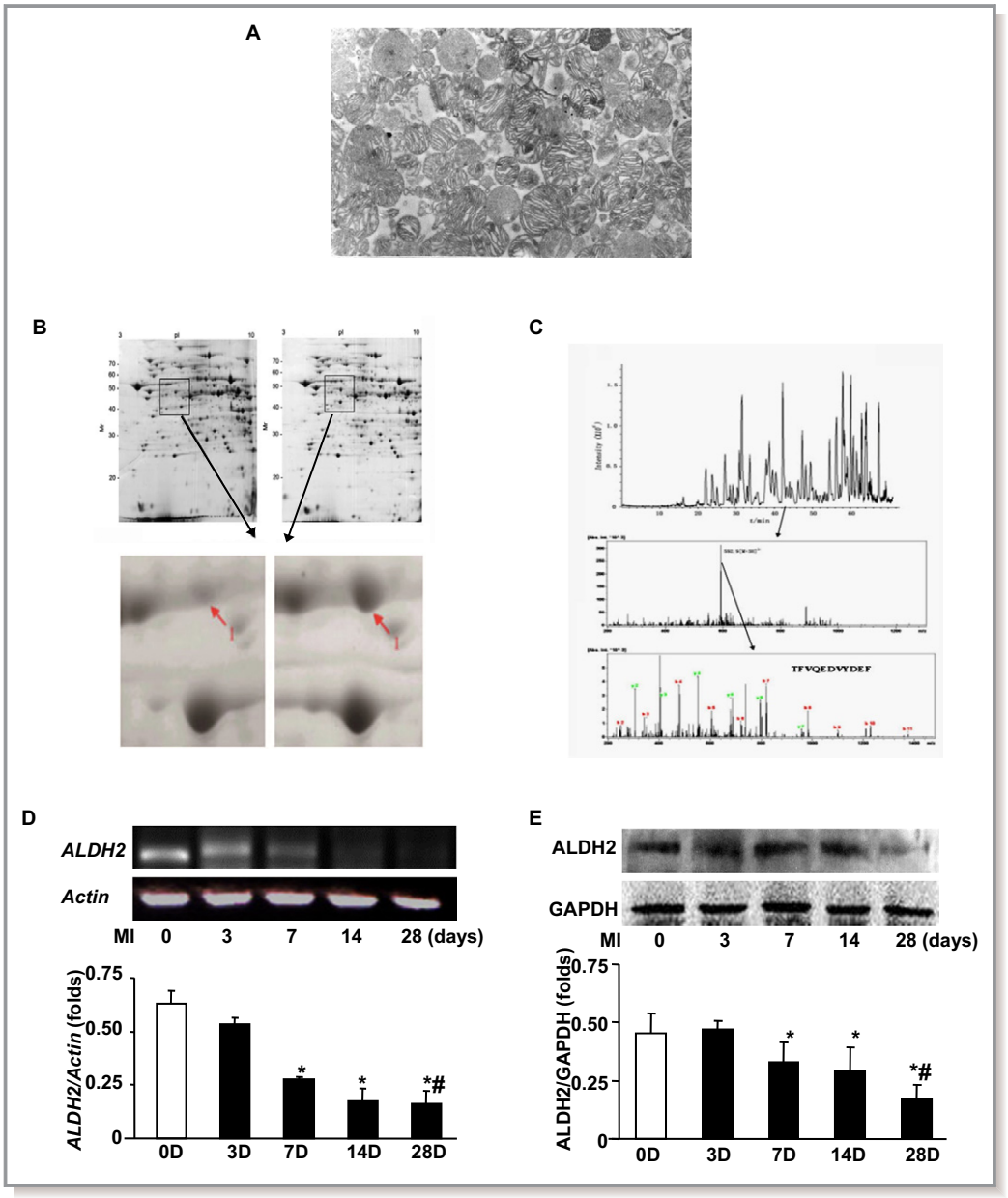

Figure 1. Cardiac mitochondrial proteome and identification of ALDH2 downregulation after MI. Mitochondrial fractions were isolated from the left ventricless of rat hearts at 4 weeks after MI or sham operation. A, Purity of isolated cardiac mitochondria evaluated by electronic microscopy. Mitochondrial fractions were isolated by a method of grade centrifugation, and the purity was 90% to 95%, evaluated by observation under an electronic microscope. B, A subfractional proteomic analysis for cardiac mitochondria. Mitochondria proteins were subjected to a 2D electrophoresis. Representative photographs are shown. Left, MI heart; Right, sham heart. C, Selection of significantly changed spots and identification by the LTQ-ESI-MS/MS. Two-dimensional electrophoresis displayed 15 protein spots that differed significantly in intensity between MI and sham hearts among ≈100 spots. The expression levels of 9 spots decreased and another 6 spots increased in MI rats compared with sham-operated rats. One of the decreased spots was identified as ALDH2. D, Confirmation of expression of *ALDH2* by RT-PCR. Rats were subjected to MI or sham operation for the indicated times. Representative photographs of RT-PCR are shown. β-Actin was used as a loading control. E, Confirmation by Western blot analyses for the expression of cardiac mitochondrial ALDH2. Rats were subjected to MI or sham operation for the indicated time. Representative photographs are shown. GAPDH was used as a loading control. ALDH2 expression was quantified as folds of β-actin or GAPDH. Data are shown as mean±SE from 9 samples. **P*<0.05 vs sham; #*P*<0.05 vs 7 days. ALDH2 indicates aldehyde dehydrogenase 2; D, days; LTQ-ESI-MS/MS, liquid chromatography electrospray ionisation tandem mass spectrometry; MI, myocardial infarction; RT-PCR, reverse transcription–polymerase chain reaction.

transfection into myocardium evaluated by X-gal staining of the LacZ vector was >50% (data not shown).[22] Small interfering RNA (siRNA) or nontargeting control (Sigma-Aldrich) was administered to mice via intraperitoneal injection.[23,24] Briefly, the siRNA of p53 or nontargeting control (Sigma-Aldrich) was administered to mice 2 days before MI via an intraperitoneal injection. Mice received 1.5 μg of siRNA per gram of body weight. Before administration, siRNA was bound to siPORT amine transfection reagent (Ambion) according to the manufacturer's instructions: siPORT amine was incubated for 30 minutes at 22°C in saline. The siPORT amine/saline mixture was then

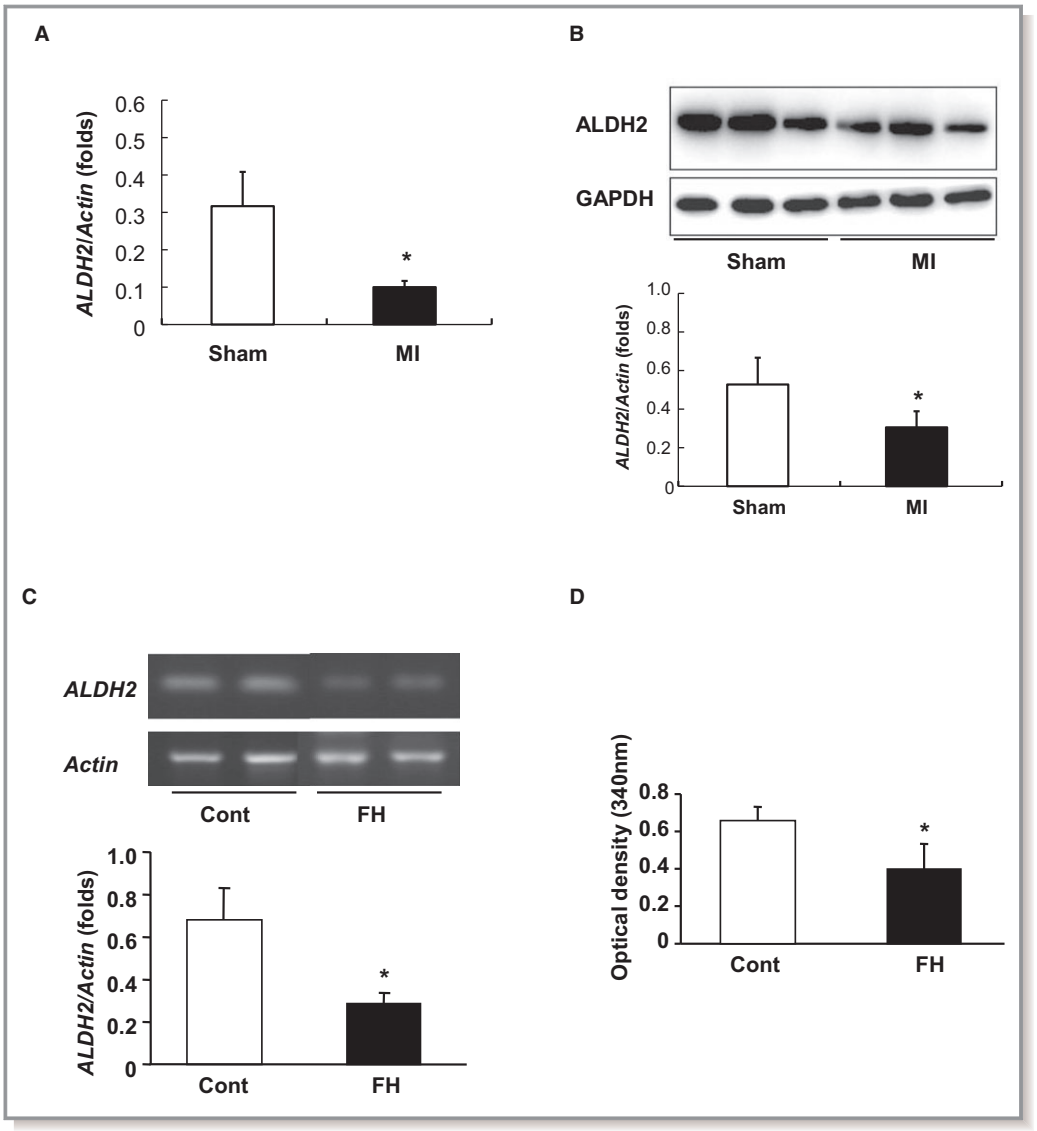

Figure 2. Downregulation of cardiac mitochondrial ALDH2 in mice after MI. Mice were subjected to MI or sham operation for 4 weeks. mRNA or mitochondria protein was prepared from hearts and subjected respectively to RT-PCR (A) and Western blot (B) analyses for ALDH2 expression. Representative photograph of Western blotting is shown. β-Actin or GAPDH was used as a loading control. ALDH2 expression was quantified as folds of β-actin or GAPDH. Data are shown as mean±SE from 9 samples. *P<0.05 vs sham. Expression of *ALDH2* (C) and ALDH2 activities (D) in human hearts. mRNA or mitochondria protein was prepared from 3 controls (aged 30 to 45 years) and 3 failing human hearts (aged 35 to 43 years). A representative photograph of RT-PCR analysis is shown. β-Actin was used as a loading control. *ALDH2* expression was quantified as folds of β-Actin, and ALDH2 activities were expressed as the initial rate of NADH production at 340 nm. Data are shown as mean±SE from 3 hearts. *P<0.05 vs control. ALDH2 indicates aldehyde dehydrogenase 2; MI, myocardial infarction; RT-PCR, reverse transcription–polymerase chain reaction.

incubated with siRNA in a 1:1 ratio for 30 minutes at 22°C. The siPORT amine/siRNA was administered at a total volume of 200 μL. The efficacy of the in vivo transfection was also evaluated by Western blot and reverse transcription–polymerase chain reaction for proteins and genes, respectively (Figure 3). All animal experimental protocols were approved by the animal care and use committee of Fudan University and in compliance with the "Guidelines for the Care and Use

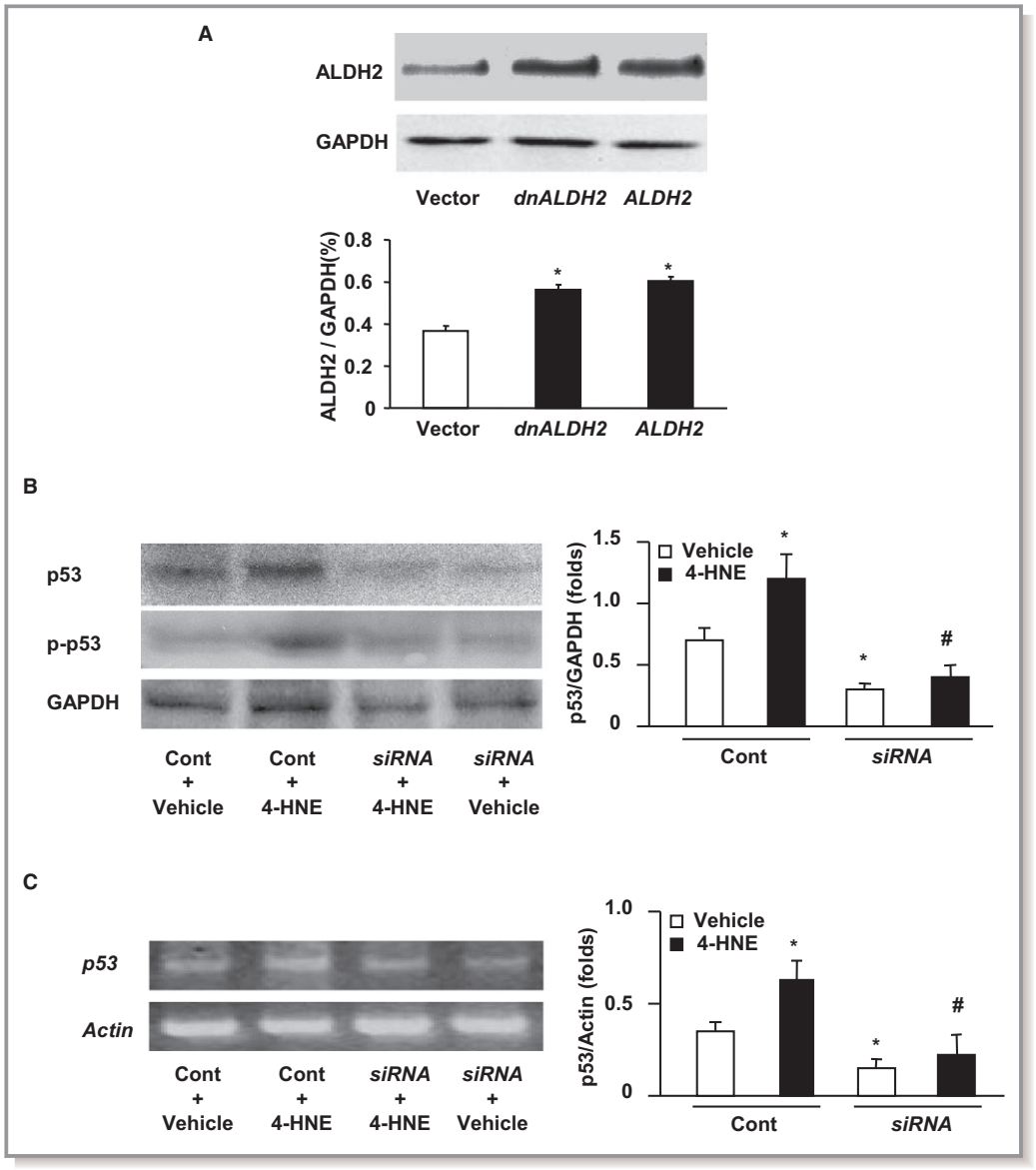

Figure 3. Analysis for cardiac ALDH2 protein expression at 2 days after in vivo gene transfection. A, Mice were subjected to the in vivo gene transfection with *ALDH2*, *dnALDH2*, or empty vector into myocardium. Two days later, the mitochondrial protein from heart tissue was subjected to Western blot analysis for ALDH2 expression. GAPDH was used as a loading control. Representative photographs are shown. Quantification of ALDH2 expression was expressed as folds of GAPDH. Data were shown as mean±SE from 9 samples. *P<0.05 vs vector. B and C, Analysis for p53 expression after treatment with siRNA. *p53* siRNA or a scramble control RNA was injected into wild type mice. The heart was isolated 2 days later and perfused with 4-HNE (10 nmol/L) or vehicle. Total proteins or mRNA from heart tissues of mice were subjected to Western blotting using the anti-p53 and phosphor-p53 antibodies (A) or RT-PCR analysis for the *p53* gene (B), respectively. Representative photographs from 3 independent experiments are shown. GAPDH and β-Actin were used as loading controls. Quantification of p53 expression was expressed as folds of GAPDH or β-Actin. Data were shown as mean±SE from 9 samples. *P<0.05 vs control–vehicle. #P<0.05 vs control–4-HNE. 4-HNE indicates 4-hydroxy-2-nonenal; ALDH2, aldehyde dehydrogenase; Cont, control; dnALDH2, dominant negative forms of *ALDH2*; siRNA, small interefering RNA.

of Laboratory Animals" published by the National Academy Press (NIH Publication No. 85-23, revised 1996).[25]

Induction of MI

MI was induced by persistent ligation of the left anterior descending artery at the same levels in animals: WT and *ALDH2*-KO mice and mice overexpressing ALDH2.[26] Sham animals underwent identical surgical procedures without left anterior descending artery ligation. Ischemic areas were controlled by Nagar-Olsen staining of the hearts at 24 hours after ligation (Figure 4).

2D Gel Electrophoresis

The 2D gel electrophoresis was carried out, first, by isoelectric focusing and, second, by SDS-PAGE. Isoelectric focusing was performed with passive in-gel rehydration of the sample followed by active in-gel rehydration of the sample in 1 dimension. Prior to SDS-PAGE, the immobilized pH gradient strips were equilibrated and sealed at the top of the 2D polyacrylamide vertical-slab precast gels. After separation performed on 12% SDS-PAGE using the Ettan DALT VI apparatus (Amersham Biosciences), the gels were stained with colloidal Coomassie blue and then scanned with an ImageScanner (Amersham Biosciences). The selected spots were sighted for further mass spectrometry identification.

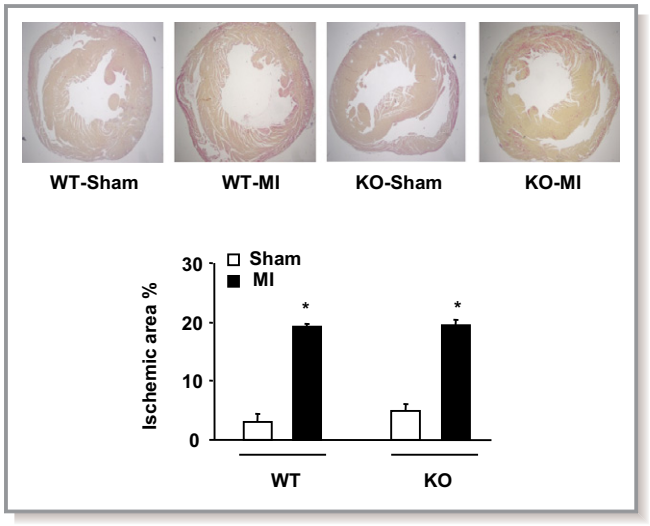

Figure 4. Analysis of ischemic area after 24 hours of MI operation. WT and *ALDH2*-KO mice were subjected to sham or MI operation. After 24 hours, the heart was removed and fixed, and the sections were subjected to Nagar-Olsen staining. Representative photographs were shown. Ischemic area was calculated as a percentage of whole left ventricle section area. Data are shown as mean±SE from 3 hearts (n=3). *P<0.01 vs respective sham-operated mice. ALDH2 indicates aldehyde dehydrogenase; KO, knockout; MI, myocardial infarction; WT, wild type.

Identification of 2D Separated Proteins

Protein spots were excised from Coomassie blue stained gels, washed with MeOH/H_2O and ACN and digested with trypsin overnight at 37°C. For mass spectrometry analysis, the peptides were separated using reverse-phase chromatography. Peptide analysis was performed on an LCQ ion trap mass spectrometer (Image master 6.0, Amersham) equipped with a gold-plated spray capillary. A mass spectrum in full-scan mode was followed by 2 tandem mass spectrometry spectra of the most abundant peptide ions.

Preparation of Human Heart Tissues

Failing human hearts were obtained from 5 end-stage HF patients admitted to our hospital for heart transplantation. Three donor hearts that could not be transplanted for technical reasons were used for controls.

Echocardiography

Echocardiography was performed using an animal-specific instrument (Vevo 770; VisualSonics Inc). Animals were anesthetized by isoflurane, and M-mode images were recorded when the heart rate of the mice was maintained at 450 to 500 beats per minute. LV ejection fraction and LV end-diastolic dimension were measured, as described previously.[21,22,26] All measurements were averaged for 5 consecutive cardiac cycles and were carried out by 3 experienced technicians who were unaware of the identities of the animal groups.

Measurement of LV Pressure

Mice were anesthetized with a cocktail of ketamine HCl (100 ng/kg) and xylazine (5 ng/kg), and the 1.4 F Millar Micro-Tip Catheter Pressure Transducer (Millar Instruments, Inc) was inserted from the right carotid artery into the aorta and then the LV of the mice. The transducer was connected to a Mac Lab system (AD Instruments) to record LV end-diastolic pressure.[21,22,25]

Langendorff Perfusion of Isolated Hearts

Mice were randomly divided into vehicle and 4-HNE perfusion groups.[25] In the vehicle group, hearts were perfused with Krebs-Henseleit buffer for 2 hours; in the 4-HNE group, hearts were perfused with 10 nmol/L 4-HNE in Krebs-Henseleit buffer for 2 hours. The concentration of 4-HNE used for Langendorff perfusion in our present study was determined by

2 steps. First, we analyzed the amount of 4-HNE in homogenizer of hearts isolated from *ALDH2*-KO mice subjected to MI for 4 weeks, and we calculated the concentration of 4-HNE (11.6±1.2 nmol/L). Second, we used 3 concentrations (5, 10, and 20 nmol/L) of 4-HNE to perfuse hearts of WT mice for 30 minutes and analyzed the injury of the heart by Nagar-Olsen staining. Perfusion with 4-HNE at the concentration of 10 nmol/L induced a significant ischemic injury to the heart; in contrast, 4-HNE at 5 and 20 nmol/L resulted slight (<5%) or severe (>50%) ischemia, respectively, neither of which is consistent with the MI experiments in our present study. Consequently, we decided to use the concentration of 10 nmol/L for 4-HNE perfusion experiments. Infarct area, cardiomyocyte apoptosis, and phosphorylation of p53 were evaluated with Nagar-Olsen staining; terminal deoxyribonucleotide transferase–mediated dUTP nick-end labeling, or TUNEL; and immunohistochemistry and Western blotting, respectively.

Cell Culture, Transfection, Anoxia, and Hypoxia Models

Cardiomyocytes were obtained from the LVs of 1-day-old neonatal rats and cultured in 60-mm dishes at a density of 1×10^5 cells/cm^2 in Dulbecco's modified Eagle's medium supplemented with 10% fetal bovine serum, as described elsewhere.[21,22,26,27] Construction and transfection of ALDH2 cDNA in adenovirus vectors were performed, as described previously.[21,22,26,28,29] Anoxia experiments were carried out by placing the cells in an anoxic incubator (GENbox; bioMérieux) for 30 minutes, 2 hours, 4 hours, and 24 hours (95% N_2 and 5% CO_2). Hypoxia experiments were performed by incubation of cultured cardiomyocytes in a hypoxic incubator (Model 9200; Wakenyaku) with 1% O_2, 5% CO_2, and 94% N_2 at 37°C for 2 or 24 hours.

Measurements of Cardiac Mitochondrial ALDH2 Enzymatic Activities

Mitochondrial fractions were obtained by a method of grade centrifugation. In brief, myocardial tissues or cultured cardiomyocytes were washed by PBS twice, then homogenized and centrifuged at 900*g* for 5 minutes to collect the supernatant. The supernatant was resuspensed with mannital-sucrose and further centrifuged at 10 000*g* for 10 minutes to collect the precipitated mitochondria. The purity of mitochondria evaluated by observation under an electronic microscope was 90% to 95%. The mitochondrial protein concentration was determined with BSA protein assay reagent. As described previously,[20] ALDH2 activity was determined by measuring the initial rate of NADH production at 340 nm using spectrophotometric assay on a spectrophotometer (Beckman) equipped with a kinetics software module. Only the linear portion of the ALDH activity curve was used for enzymatic activity analysis.

Histology

Heart tissues from the ischemic region were fixed in 10% formalin and embedded in paraffin or frozen in liquid nitrogen; sectioned at 4-μm thickness; and stained with Masson trichrome, Nagar-Olsen, and immunohistochemical methods using anti-p53 (#2524; Cell Signaling Technology), phosphor-p53 (FL-393, #sc-6243), poly-(APD-ribose) polymerase (PARP) and 4-HNE antibodies (Santa Cruz Biotechnology Inc). The immunostaining of p53 was performed according to the immunohistochemistry protocol from Cell Signaling Technology using the p53 antibody diluted by 1:2000. To confirm the specific staining for p53 and phosphor-p53, we also stained heart tissues of p53 knockout mice (kindly provided by Dr. Xuemei Tong at Shanghai Jiaotong University, Shanghai, China) using the similar p53 and phosphor-p53 antibodies (Figure 5). Digital photographs were taken at magnification ×20, ×100, or ×400, and 5 random high-power fields from each section were chosen and quantified in a blinded manner. Infarct size, ischemic cardiomyocytes, p53, phosphor-p53, PARP, and 4-HNE were measured in 5 sections from each heart, and the mean value was expressed.

Analyses of Apoptosis

Apoptosis was evaluated by TUNEL assay and fluorescence-activated cell sorting (FACS). TUNEL analyses for ischemic tissue or cultured cardiomyocytes were performed according to the manufacturer's protocol (In Situ apoptosis detection kit; Takara). FACS analysis for apoptosis was performed as follows: cells were washed with PBS, resuspended in 1X Annexin Binding Buffer (BD PharMingen), and incubated with annexin V-fluorescence isothiocyanate (FITC; BD PharMingen) and propidium iodide. Apoptotic cells were measured by Becton Dickinson FACS 18 Caliber bench-top flow cytometer (Image master 6.0). Apoptosis was also evaluated by a transmission electron microscopy and DNA laddering. For DNA fragmentation, total DNA was extracted from cardiomyocytes using a DNA binding column (BioDev Co), washed twice with rinsing fluid, dried, diluted in Tris-EDTA buffer, and separated by agarose gel. DNA fragments were visualized with ultraviolet light.

Western Blot

Proteins from heart tissues and cardiomyocytes were size fractionated by SDS-PAGE and transferred to Immobilon-P membranes (Millipore). The blotted membranes were incubated with antibodies against ALDH2, p53, phosphor-p53, ERKs,

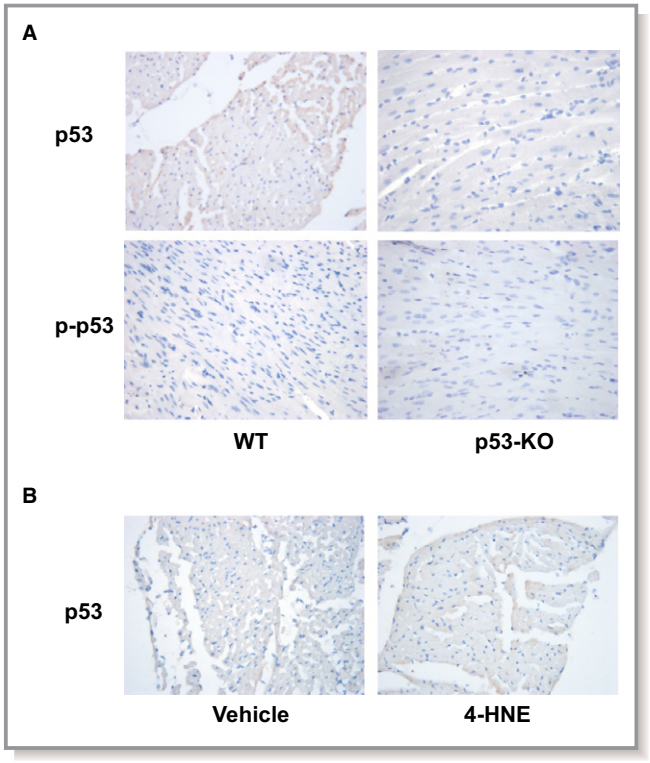

Figure 5. Immunohistochemistry staining of phosphor-p53 and total p53. A, Heart tissues from wild type and p53 knockout mice were fixed in 10% formalin and embedded in paraffin, sectioned at 4-μm thickness, and stained with immunohistochemical methods using anti-p53 and phosphor-p53, respectively. The immunostaining of p53 was performed according to the manufacturer's immunohistochemistry protocol using the p53 antibody diluted by 1:2000. Digital photographs were taken at magnification ×400, and p53 and phosphor-p53 were observed in 5 sections from each heart; the representative photographs are shown. B, Total p53 expression in isolated heart. Isolated hearts were perfused with 4-HNE (10 nmol/L) or vehicle for 2 hours. Representative staining for p53 is shown. 4-HNE indicates 4-hydroxy-2-nonenal; KO, knockout; p-p53, phosphor-p53; WT, wild type.

phosphor-ERKs, JNK, phosphor-JNK, HSP70, or GAPDH (Santa Cruz Biotechnology Inc). Immunoreactivity was detected using an enhanced chemiluminescence reaction system (Amersham Pharmacia Biotech).

Reverse Transcription–Polymerase Chain Reaction

Total RNA was isolated from the LV tissues or cells using TRIzol reagent (15596-018; Gibco BRL). The expression of *ALDH2* and p53 at mRNA levels was evaluated using reverse transcription–polymerase chain reaction. The primers were as follows (forward/reverse): *ALDH2*, agagaggacgcttgctgaac/gcagggcctatcttccaaat; *p53*, 5′-tggctcctccccaacatcttatc-3′/5′-cttcctctgtccgacggtctctc-3′. The polymerase chain reaction products were subject to electrophoresis on 1.5% agarose gels, scanned, and semiquantified using Image-Quant software (Kodak 1D V3.53).

Statistical Analysis

All values are presented as mean±SE. Multiple group comparison was performed by 1- or 2-way ANOVA followed by the Bonferroni procedure for comparison of means. Comparisons between 2 groups were analyzed with the unpaired 2-tailed Student *t* test. Values of $P<0.05$ were considered statistically significant.

Results

Effects of *ALDH2* Modulation on Cardiac Dilation, Dysfunction, and Apoptosis in MI Mice

To elucidate the role of ALDH2 in HF after MI, we produced MI in WT and *ALDH2*-KO mice. *ALDH2*-KO mice showed no significant differences in body weight, blood pressure, heart rate, and echocardiographic parameters compared with WT mice at basal conditions (Table 2). Ischemic injury at early stage (24 hours) after MI was evaluated by Nagar-Olsen staining of the hearts and showed no significant difference between WT and *ALDH2*-KO mice (Figure 4). At 4 weeks after MI, however, the LV cavity, LV end-diastolic pressure, and infarct size were significantly greater and LV ejection fraction was significantly lower in *ALDH2*-KO mice than in WT mice (Figure 6A and 6B). Meanwhile, TUNEL (Figure 6C) and immunohistochemical staining with PARP (Figure 6D) showed that the number of apoptotic cells in the noninfarction LV area was significantly higher in *ALDH2*-KO mice than in WT mice. In contrast, overexpression of *ALDH2* in myocardium of WT mice by injecting adenovirus vectors encoding the murine *ALDH2* gene 2 days prior to MI significantly reduced the LV cavity and LV end-diastolic pressure and increased the LV ejection fraction compared with WT mice injected with empty vector (Figure 7A; Table 3). Infarct size (Figure 7B) and the numbers of TUNEL- or PARP-positive cardiomyocytes (Figure 7C and 7D) were also lower in *ALDH2*-injected hearts than in empty vector–injected hearts. These results collectively suggest that ALDH2 protects against HF after MI partly by reducing cardiomyocyte apoptosis.

Effects of *ALDH2* Modulation on Anoxia-Induced Cardiomyocyte Apoptosis

The effects of *ALDH2* modulation on apoptosis were also observed in cultured cardiomyocytes that underwent anoxia injury. The spectrophotometric assays revealed that the ALDH2 activity of cardiomyocytes was decreased in a time-dependent manner during anoxia (Figure 8A), which was

Table 2. Body Weight, Blood Pressure, Heart Rate, and Echocardiographic Parameters at Basal State

	WT	ALDH2-KO	*P* Value
BW, g	25.9±3.2	26.7±4.0	NS
BP, mm Hg	95.6±6.5	98.1±7.2	NS
HR, bpm	489.3±35.2	494.7±40.5	NS
LVAWd, mm	0.76±0.03	0.78±0.04	NS
LVPWd	0.75±0.04	0.77±0.02	NS
LVESD, mm	1.35±0.18	1.39±0.20	NS
LVEDD, mm	2.97±0.23	3.18±0.41	NS
LVEF, %	80±5.3	81±6.7	NS

Twelve-week-old wild type and ALDH2-KO mice at basal condition were subjected to echocardiographic analysis. Data are shown as mean±SE of 10 mice. ALDH2 indicates aldehyde dehydrogenase2; BP, blood pressure; BW, body weight; HR, heart rate; KO, knockout; LVAWd, left ventricle anterior wall thickness at diastole; LVPWd, left ventricular posterior wall thickness at diastole; LVEDD, left ventricular end-diastolic dimension; LVESD, left ventricular end-systolic dimension; LVEF, left ventricular ejection fraction; NS, not significant.

associated with an increase in apoptosis (Figure 8B). To explore the effects of modulating *ALDH2* on cardiomyocyte apoptosis, an *ALDH2* or *dnALDH2* gene that was constructed by a substitution of Glu with Lys at the 14th last codon of murine *ALDH2*[28] was introduced into cardiomyocytes. ALDH2 activity was significantly decreased in the empty vector–transfected cells after anoxia (Figure 8C), and the decrease of ALDH2 activity was alleviated by *ALDH2* but aggravated by *dnALDH2* transfection (Figure 8C). As expected, anoxia-induced cardiomyocyte apoptosis was attenuated by *ALDH2* but aggravated by *dnALDH2* transfection (Figure 8D). These results suggest that ALDH2 could be a major player in protection of cardiomyocytes from anoxia-induced apoptosis.

Detoxifying the 4-HNE as the Major Mechanism of ALDH2 Effects

4-HNE is one of the most toxic aldehydes produced during lipid peroxidation.[30,31] Because 4-HNE is detoxified by ALDH2, we postulated that 4-HNE might be involved in ALDH2-induced

Table 3. Summary of Echocardiographic Data in Mice Subjected to In Vivo Gene Transfer With Empty Vector or *ALDH2* Into Myocardium and MI for 28 Days

	Vector	*ALDH2*	*P* Value
IVSd	0.4900±0.2074	0.7975±0.2124	0.084
LVIDd	4.2550±0.2356	3.3550±0.5337	0.022
LVPWd	0.8840±0.1168	1.4267±0.3683	0.019
IVSs	0.5767±0.4159	1.5333±0.1935	0.023
LVIDs	3.0200±0.5243	1.4867±0.1537	0.008
LVPWs	1.3650±0.1921	1.7050±0.5092	0.258
RWTs	0.5400±0.2771	1.2667±0.5181	0.099
RWTd	0.2000±0.0361	0.4633±0.1474	0.040
LVVold	81.300±10.629	47.130±17.709	0.016
LVVols	30.478±17.151	5.9900±1.5062	0.061
LV mass uncorrected	102.13±20.929	127.39±29.352	0.174
LV mass corrected	81.702±16.743	101.92±23.472	0.174
LVESD	2.9300±0.5945	1.5750±0.3543	0.008
Stroke volume	49.215±13.028	35.255±4.6366	0.090

Adenovirus vectors encoding *ALDH2* or empty vectors were infused into myocardium of wild type mice. After 2 days, mice were subjected to MI. Echocardiographic analysis was carried out at 4 weeks after MI. Data are shown as mean±SE of 5 mice. ALDH2 indicates aldehyde dehydrogenase 2; IVSd: interventricular septal dimension in diastole; IVSs: interventricular septal dimension in systole; LV, left ventricle; LVIDd, left ventricular internal dimension at end-diastole; LVIDs, left ventricular internal diameter at end-systole; LVESD, left ventricular end-systolic dimension; LVPWs, left ventricle posterior wall thickness at systole; LVV, left ventricular volume; LVVold, left ventricular volume during diastole; LVVols, left ventricular volume during systole; MI, myocardial infarction; RWTd, relative wall thickness at diastole; RWTs, relative wall thickness at systole; Vector, empty vector.

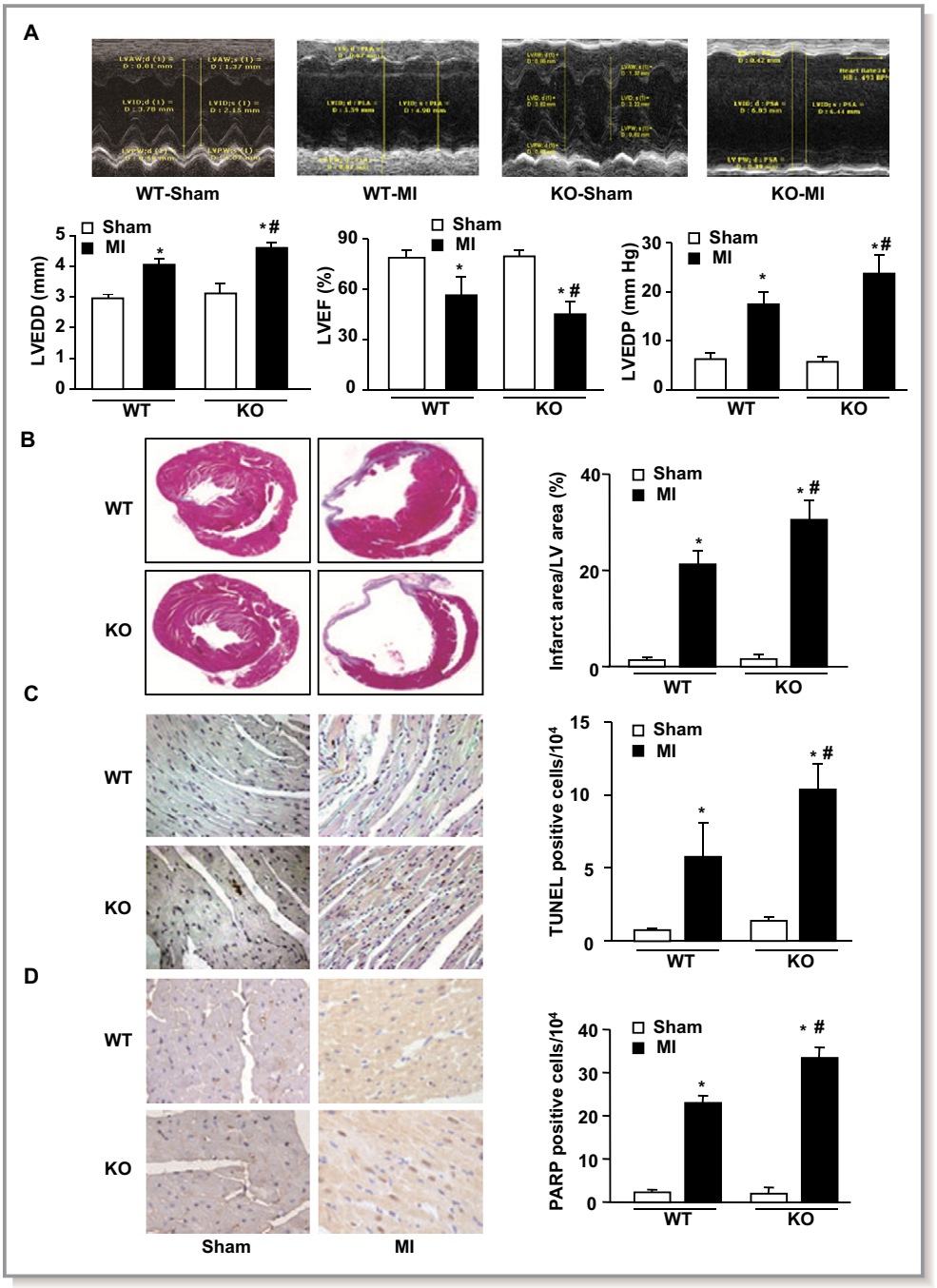

Figure 6. LV dilation, dysfunction, infarct size and cardiomyocyte death after MI in ALDH2-deficient mice. MI was produced in adult male WT and *ALDH2*-KO mice, and LV morphology, function, infarct size, and apoptosis were examined at 4 weeks. A, LV morphology and function. Representative M-mode echocardiographic photographs of LV and quantified LVEDD, LVEF, and LVEDP values are shown. B, Infarct size. Representative photographs of Masson trichrome–stained heart sections from sham-operated and MI mice are shown. Infarcted area was determined by measuring fibrosis area and is expressed as a percentage of the whole LV area. Apoptosis evaluated by TUNEL (C) and immunostaining against PARP (D). Representative photographs are shown. Brown nuclei indicate TUNEL- or PARP-positive cells. Apoptotic cells were counted as the numbers of positive cells per 10^4 cells in the whole LV area. Data are shown as mean±SE from 5 mice. *P<0.05 vs sham in same genotype mice. #P<0.05 vs MI in WT mice. ALDH2 indicates aldehyde dehydrogenase 2; KO, knockout; LV, left ventricle; LVEDD, left ventricular end-diastolic dimension; LVEDP, left ventricular end-diastolic pressure; LVEF, left ventricular ejection fraction; MI, myocardial infarction; PARP, poly-(APD-ribose) polymerase; TUNEL, terminal deoxyribonucleotide transferase–mediated dUTP nick-end labeling; WT, wild type.

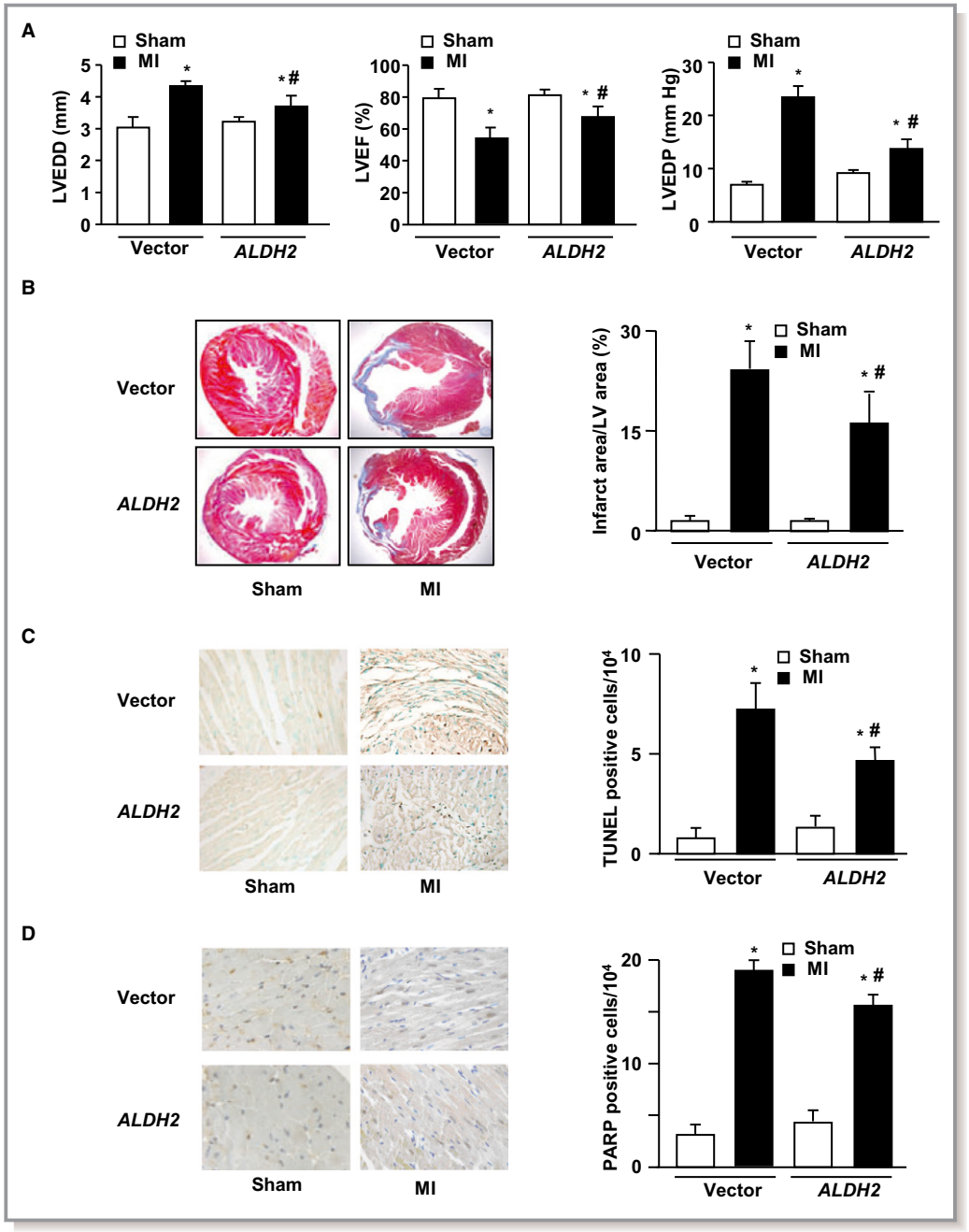

Figure 7. Protection of the heart by overexpression of *ALDH2*. Adenovirus vectors encoding *ALDH2* or empty vectors were infused into myocardium of WT mice. After 2 days, mice were subjected to MI or sham for 4 weeks. A, Quantified LVEDD, LVEF, and LVEDP by echocardiography and catheterization. B, Infarct size. Representative photographs of Masson trichrome staining are shown. TUNEL (C) and immunostaining for PARP (D). Representative photographs are shown. Apoptotic cells were calculated as the numbers of positive cells per 10^4 cells in the whole LV section. Data are shown as mean±SE from 5 hearts. *P<0.05 vs respective sham group, #P<0.05 vs MI mice with vector transfection. ALDH2 indicates aldehyde dehydrogenase 2; LVEDD, left ventricular end-diastolic dimension; LVEDP, left ventricular end-diastolic pressure; LVEF, left ventricular ejection fraction; MI, myocardial infarction; PARP, poly-(APD-ribose) polymerase; TUNEL, terminal deoxyribonucleotide transferase–mediated dUTP nick-end labeling; Vector, empty vector; WT, wild type.

cardiac protection during the development of MI in vivo and in ALDH2-induced antiapoptotic effect on hypoxic cardiomyocytes in vitro.

Our immunohistochemical staining results showed that 4-HNE was almost absent in the LVs of sham-operated WT mice but was readily observed in the border region of infarcted

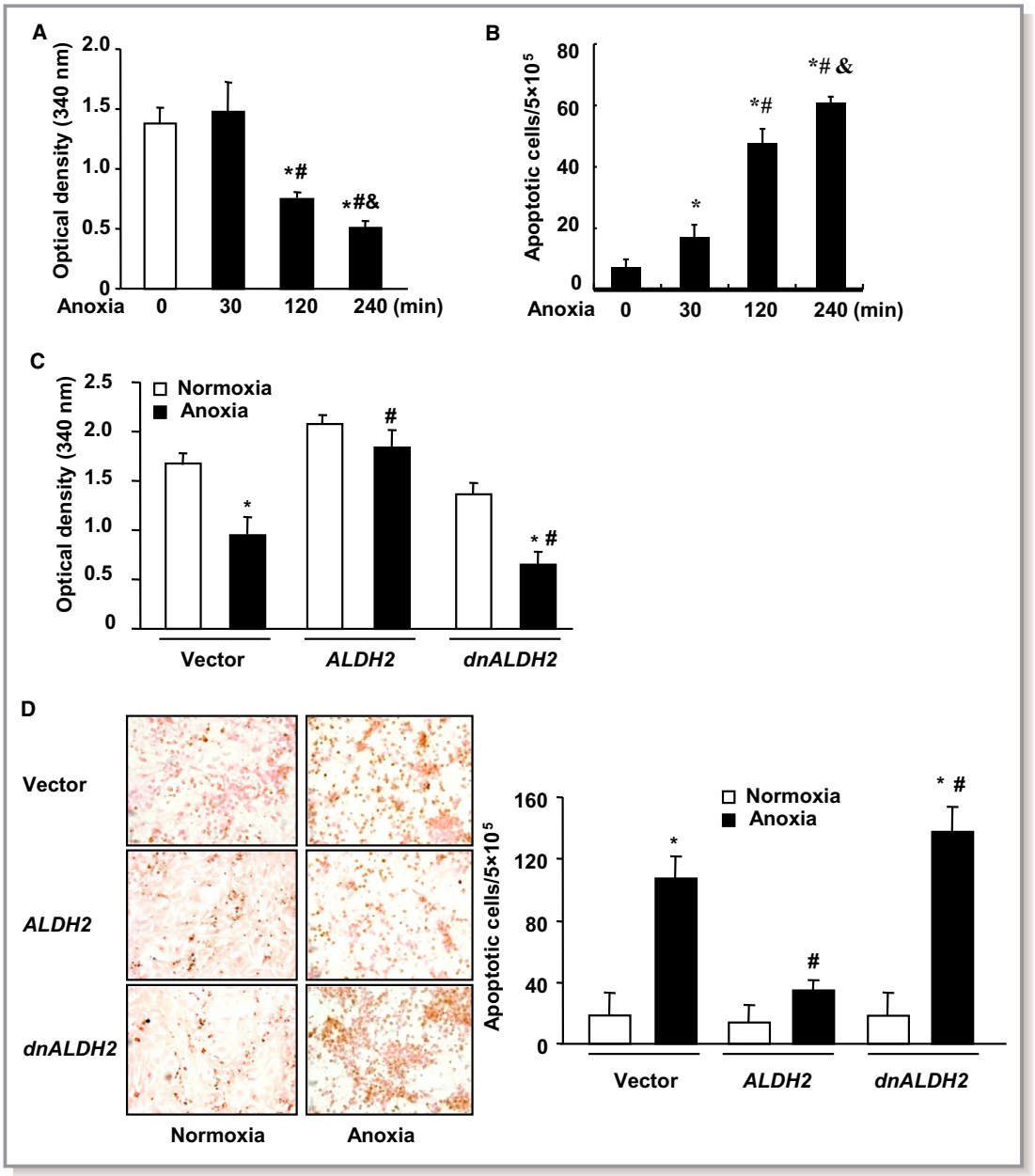

Figure 8. Protection of cultured cardiomyocytes by ALDH2. A, Anoxia-induced changes of ALDH2 activities in cardiomyocytes. Cultured cardiomyocytes were exposed to anoxia for the indicated times. Data are shown as mean±SE from 9 samples. *P<0.05 vs control (0 minute). #P<0.05 vs anoxia for 30 minutes. &P<0.05 vs anoxia for 120 minutes. B, Anoxia-induced apoptosis in cardiomyocytes. Cultured cardiomyocytes were exposed to anoxia for the indicated times. Apoptosis was analyzed by FACS. Data are shown as mean±SE from 9 samples. *P<0.05 vs control (0). #P<0.05 vs treatment with anoxia for 30 minutes. &P<0.05 vs anoxia for 2 hours. C, Effects of *ALDH2* transfection on ALDH2 activities. Cardiomyocytes were transfected with empty vector, *ALDH2* or *dnALDH2* and exposed to anoxia or normoxia for 2 hours. Data are shown as mean±SE from 9 samples. *P<0.01 vs respective normoxia. #P<0.05 vs empty vector with anoxia. D, Effects of *ALDH2* transfection on apoptosis. Cardiomyocytes transfected with empty vector, *ALDH2*, or *dnALDH2* were subjected to anoxia for 24 hours. Apoptosis was detected by TUNEL (brown nuclei). Representative photographs are shown. TUNEL staining was quantified as the number of apoptotic cells per 5×10^5 cells. Data are shown as mean±SE of 9 samples. *P<0.01 vs respective normoxia. #P<0.05 vs vector with anoxia. ALDH2 indicates aldehyde dehydrogenase 2; dnALDH2, dominant negative forms of *ALDH2*; FACS, fluorescence-activated cell sorting; TUNEL, terminal deoxyribonucleotide transferase–mediated dUTP nick-end labeling; Vector, empty vector.

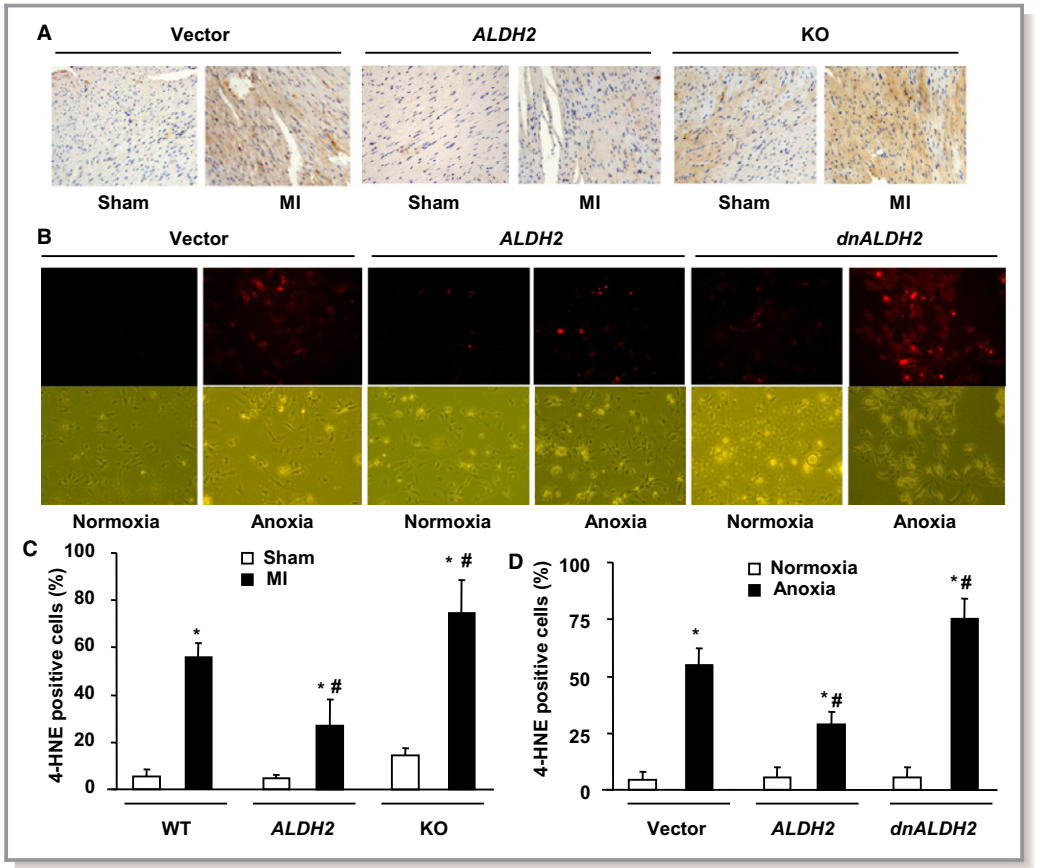

Figure 9. Measurement of 4-HNE in myocardium and cardiomyocytes. A, Distribution of 4-HNE in myocardium. WT mice with cardiac overexpression of *ALDH2* or empty vector and *ALDH2*-KO mice were subjected to MI or sham operation for 4 weeks. 4-HNE was stained with anti 4-HNE antibodies. Representative photographs from 5 hearts are shown. Brown indicates 4-HNE positive signals. B, Detection of 4-HNE in cardiomyocytes. Cultured cardiomyocytes were transfected with *ALDH2*, *dnALDH2*, or empty vector and stimulated with anoxia or normoxia. 4-HNE was detected by immunofluorescent staining method under confocal scanning laser microscopy. Representative photographs are shown. Top, staining of 4-HNE (red). Bottom, cells under the optical microscopy. Quantification of 4-HNE in myocardium (C) and cardiomyocytes (D). 4-HNE–positive cells were presented as percentage of total cells. Data are shown as mean±SE of 5 hearts or 15 cardiomyocytes. **P*<0.01 vs respective sham or normoxia. #*P*<0.05 vs WT with MI or vector with anoxia. 4-HNE indicates 4-hydroxy-2-nonenal; ALDH2, aldehyde dehydrogenase 2; dnALDH2, dominant negative forms of *ALDH2*; KO, knockout; MI, myocardial infarction; Vector, empty vector; WT, wild type.

myocardium of the WT mice (Figure 9A and 9C). The increase in 4-HNE after MI was significantly attenuated by transfection with *ALDH2*. 4-HNE was detectable even in the LVs of sham-operated *ALDH2*-KO mice and upregulated more significantly in the LVs of *ALDH2*-KO mice after MI (Figure 9A and 9C). In cultured cardiomyocytes, anoxia enhanced production of 4-HNE, which was further increased by *dnALDH2* but decreased by *ALDH2* transfection (Figure 9B and 9D), consistent with the changes of cardiomyocyte apoptosis.

These results suggest that the protection of cardiomyocytes by ALDH2 is associated with detoxification of 4-HNE. To observe its direct effects, 4-HNE was perfused into the isolated murine heart in Langendorff mode. Perfusion with 4-HNE induced a significant myocardial injury (Figure 10A and 10B) and apoptosis (Figure 10A and 10C). Furthermore, treatment with 4-HNE significantly induced the karyopyknosis and the DNA fragmentation in cultured cardiomyocytes (Figure 10D and 10E). Taken together, the accumulation of 4-HNE as a consequence of ALDH2 downregulation could induce cardiomyocyte apoptosis, thereby promoting LV dilation and dysfunction after MI.

Involvement of p53 in the Effects of ALDH2 and 4-HNE on Cardiomyocytes

We further examined the potential signaling pathway related to ALDH2-downregulation- and 4-HNE-upregulation-induced cardiomyocyte apoptosis. It is known that the tumor suppressor p53 regulates cardiomyocyte apoptosis and is

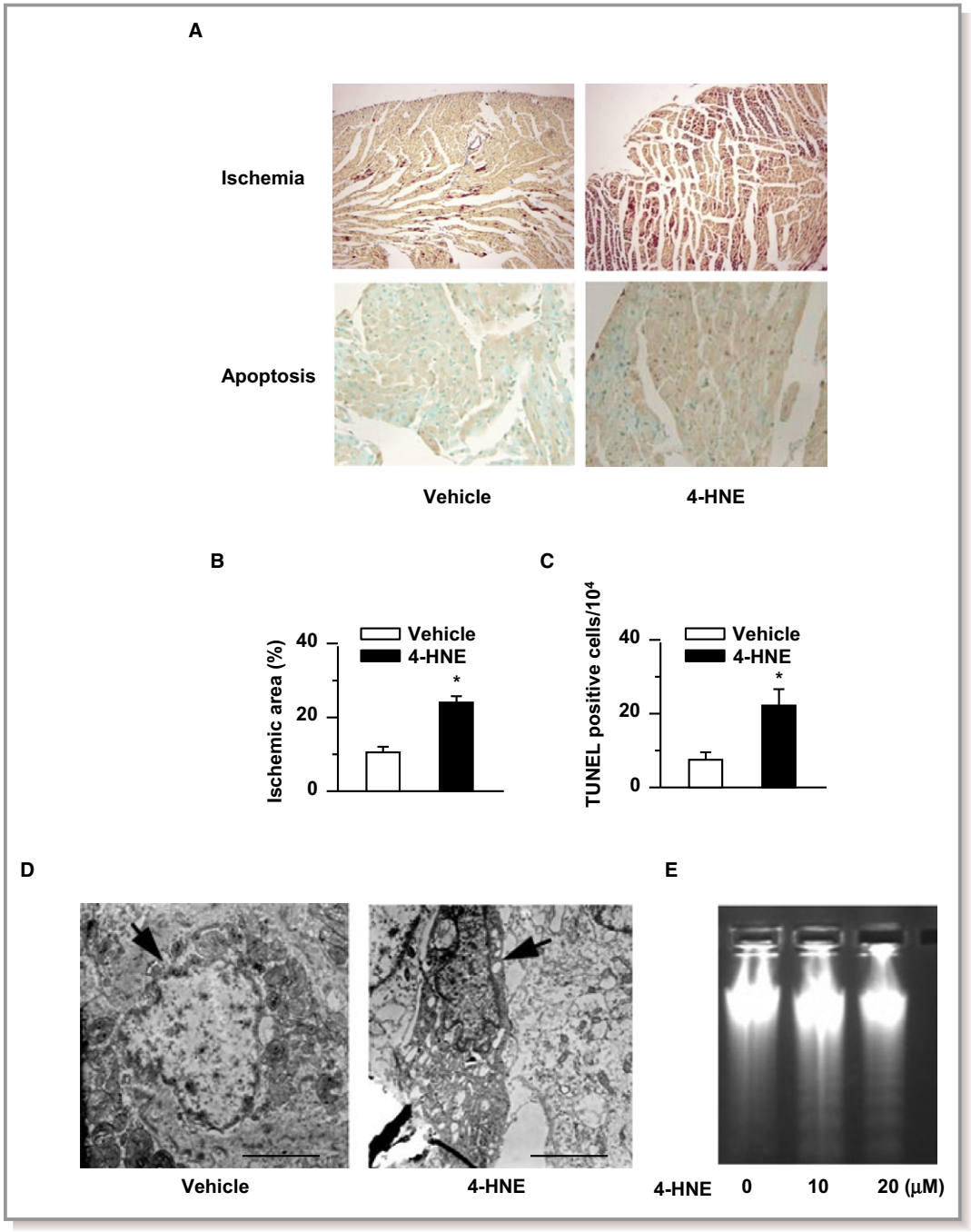

Figure 10. 4-HNE–induced cardiomyocyte injury and apoptosis. A, Myocardial injury and apoptosis induced by 4-HNE. The isolated murine heart was perfused with 4-HNE (10 nmol/L) or vehicle under a Langendorff perfusion system for 2 hours. Ischemic area and apoptosis were analyzed by Nagar-Olsen staining and TUNEL method, respectively. Representative photographs are shown. Top, Nagar-Olsen staining, red signals indicate ischemic area. Bottom, TUNEL, brown nuclei indicate apoptosis. Quantification of ischemic area (B) and apoptosis (C). Ischemic area was calculated as percentage of whole LV area. Apoptotic cells were expressed as the numbers of TUNEL-positive nuclei per 10^4 cells in whole LV area. Data are shown as mean±SE from 5 hearts. *P<0.01 vs vehicle. D, Apoptotic bodies in cultured cardiomyocytes. Cardiomyocytes treated with 4-HNE or vehicle for 24 hours were examined by a transmission electron microscopy. Representative photographs from 9 samples are shown (scale bar = 2 μm). Arrows indicate the nuclei, which showed significant karyopyknosis in 4-HNE- but not vehicle-treated cells. E, DNA fragmentation. Cardiomyocytes were treated with indicated concentrations of 4-HNE for 24 hours. A representative photograph of 9 samples is shown. 4-HNE indicates 4-hydroxy-2-nonenal; LV, left ventricle; TUNEL, terminal deoxyribonucleotide transferase–mediated dUTP nick-end labeling.

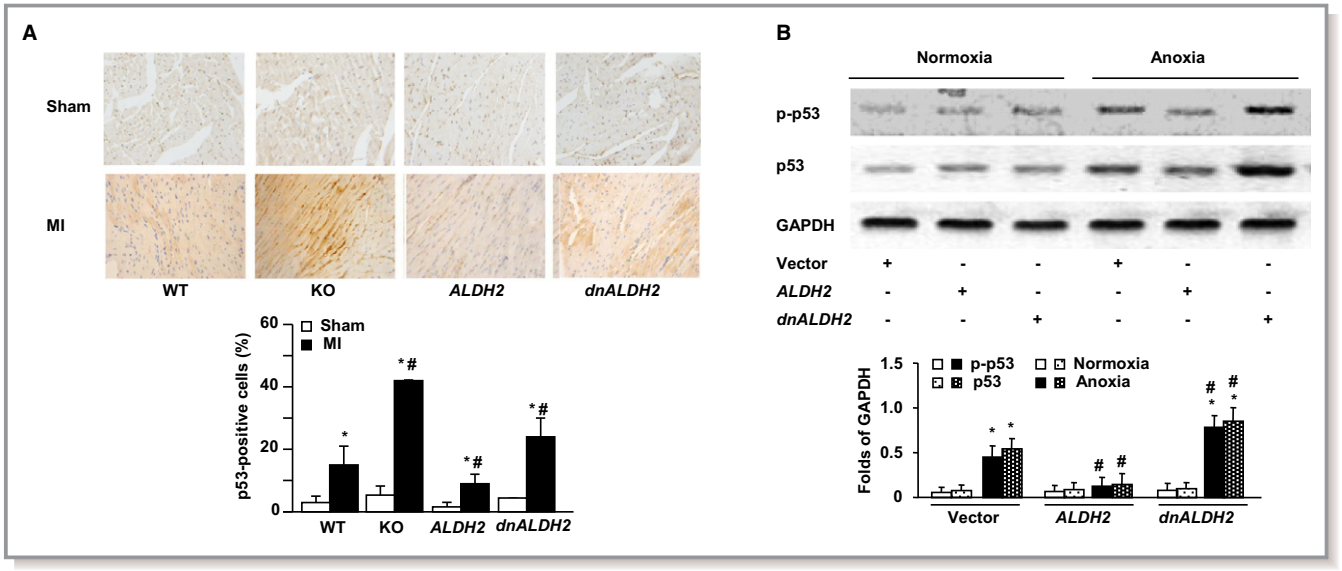

Figure 11. Involvement of p53 in ALDH2- and 4-HNE–induced cardiac injuries. A, Detection of p53 by immunohistochemistry in myocardium. Mice were subjected to sham or MI for 24 hours. p53 was stained by an anti-p53 antibody (brown). Representative photographs are shown. p53 positive cells were calculated in whole LV section and expressed as percentage of total cells. Data are shown as mean±SE of 5 hearts. *P<0.05 vs respective sham. #P<0.05 vs WT with MI. B, Western blot analyses for expression and phosphorylation of p53 in cardiomyocytes. Cultured cardiomyocytes were transfected with empty vector, *ALDH2*, or *dnALDH2* and exposed to anoxia or normoxia for 2 hours (for p-p53) or 24 hours (for p53 protein expression). GAPDH was used as a loading control. Representative photographs are shown. The band densities were determined by scanning each band with a densitometer, and p-p53 and p53 are expressed relative to bands of GAPDH (folds). Data are shown as mean±SE from 15 samples. *P<0.01 vs respective normoxia. #P<0.05 vs empty vector with hypoxia. C, Effects of ALDH2 on phosphorylation and expression of p53 under hypoxia condition. Cultured cardiomyocytes were transfected with empty vector, *ALDH2*, or *dnALDH2* and exposed to hypoxia or vehicle for 2 or 24 hours. p53 expression and phosphorylation levels were examined by Western blotting using an anti-p53 or p-p53 antibody. Representative photographs from 9 samples are shown. ALDH2 expression in cultured cardiomyocytes overexpressing p53. Cultured cardiomyocytes of neonatal rats were transfected with adenoviral vectors encoding *p53* or empty vector or without transfection and exposed to anoxia or normoxia for 24 hours. mRNA or mitochondria protein was subjected respectively to reverse transcription–polymerase chain reaction (D) and Western blot (E) analyses for ALDH2 expression. Representative photograph of Western blotting is shown. β-Actin or GAPDH was used as a loading control. ALDH2 expression was quantified as folds of β-Actin or GAPDH,. Data are shown as mean±SE from 9 samples. *P<0.05 vs control with normoxia. F, 4-HNE–induced p53 phosphorylation in isolated heart. Isolated hearts were perfused with 4-HNE (10 nmol/L) or vehicle for 2 hours. Representative staining for p-p53 (brown) is shown. The p-p53 positive cells were calculated in whole LV sections and expressed as percentage of total cells. Data are shown as mean±SE of 5 hearts. *P<0.05 vs vehicle. G, Effects of a p53 inhibitor on 4-HNE–induced cardiomyocyte apoptosis. Cultured cardiomyocytes were pretreated with Pft or vehicle (negative) for 30 minutes and then incubated with 4-HNE (10 μmol/L) or vehicle for 24 hours. Apoptosis was examined by TUNEL method. Representative photographs are shown. Brown indicates the apoptotic nuclei. TUNEL-positive cells were calculated as percentage of total cells in whole dish and expressed as mean±SE of 15 samples. *P<0.01 vs respective vehicle. #P<0.05 vs 4-HNE without Pft. H, Effects of *p53* siRNA on 4-HNE–induced myocardial injury. The *p53* siRNA or a scramble control RNA (control) was injected into WT mice. The heart was isolated 2 days later and perfused with 4-HNE (10 nmol/L) or vehicle for 2 hours. Apoptosis was evaluated by TUNEL. Representative photographs are shown. Apoptotic cells were quantified as the numbers of TUNEL-positive cells per 10^4 cells in whole LV section. Data are shown as mean±SE of 5 hearts. *P<0.05 vs respective vehicle. #P<0.05 vs 4-HNE with the scramble control RNA. 4-HNE indicates 4-hydroxy-2-nonenal; ALDH2, aldehyde dehydrogenase 2; Cont, control; dnALDH2, dominant negative forms of *ALDH2*; KO, knockout; LV, left ventricle; MI, myocardial infarction; p-p53, phosphor-p53; TUNEL, terminal deoxyribonucleotide transferase–mediated dUTP nick-end labeling; Vector, empty vector; WT, wild type.

profoundly involved in the development of HF[2,21,26,32]; therefore, we examined whether modulation of ALDH2 could affect p53 expression and phosphorylation. Histological staining results showed that the protein levels of p53 were significantly increased in *ALDH2*-KO and *dnALDH2*-transfected hearts but decreased in *ALDH2*-transfected hearts compared with hearts of WT mice (Figure 11A). In addition, Western blot analysis revealed that, in response to anoxia, both the expression and phosphorylation levels of p53 in cardiomyocytes were significantly increased by *dnALDH2* but suppressed by *ALDH2* compared with empty vector transfection (Figure 11B). Another experiment under hypoxia conditions revealed the similar results to those under anoxia conditions (Figure 11C). These results suggest that ALDH2 regulates the

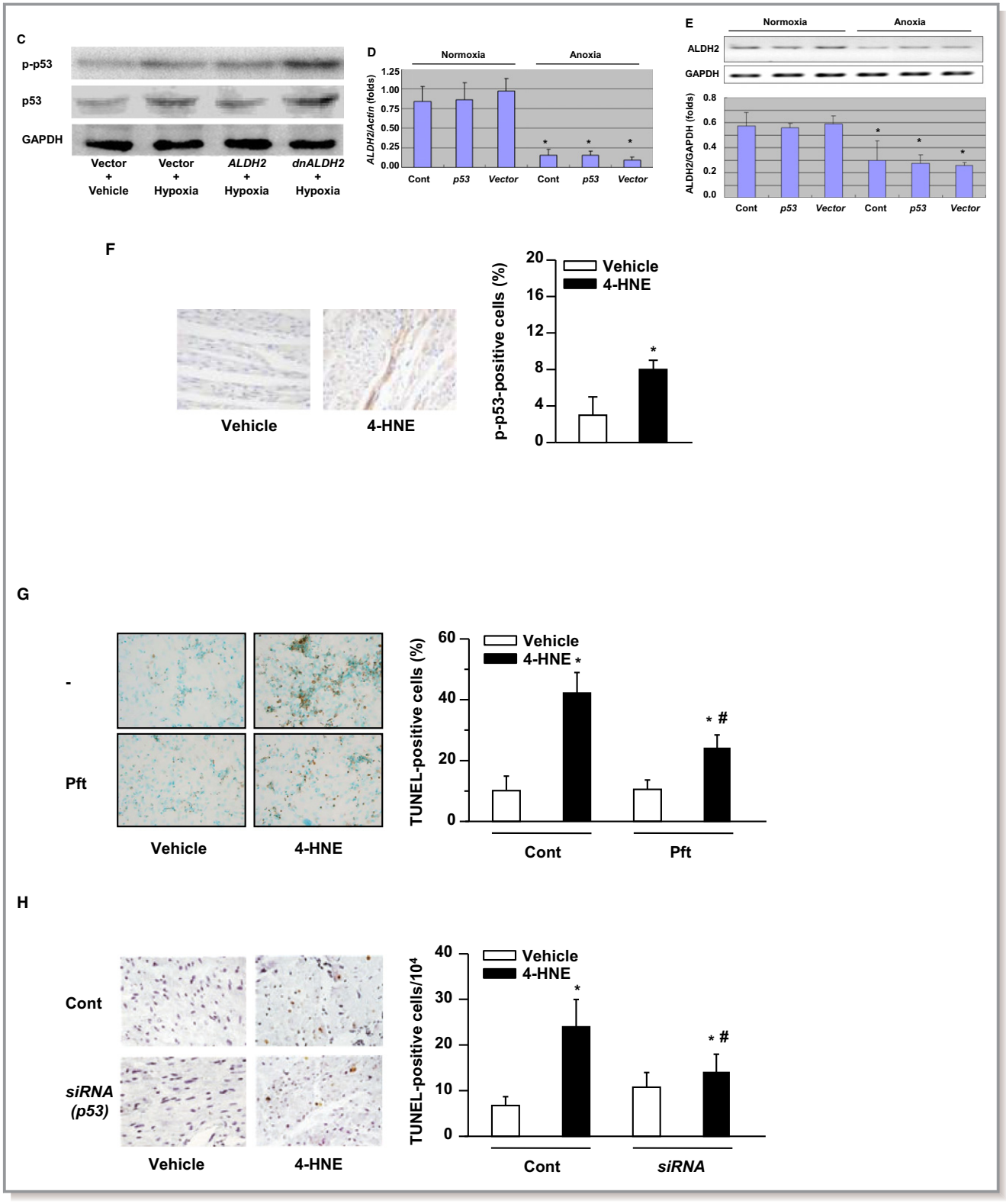

Figure 11. Continued.

expression and phosphorylation of p53 in cardiomyocytes. In turn, to understand whether p53 affects ALDH2, we examined the expression of ALDH2 after transfecting p53 into cardiomyocytes. The expression of ALDH2 at both mRNA (Figure 11D) and protein (Figure 11E) levels was not affected by transfection of p53.

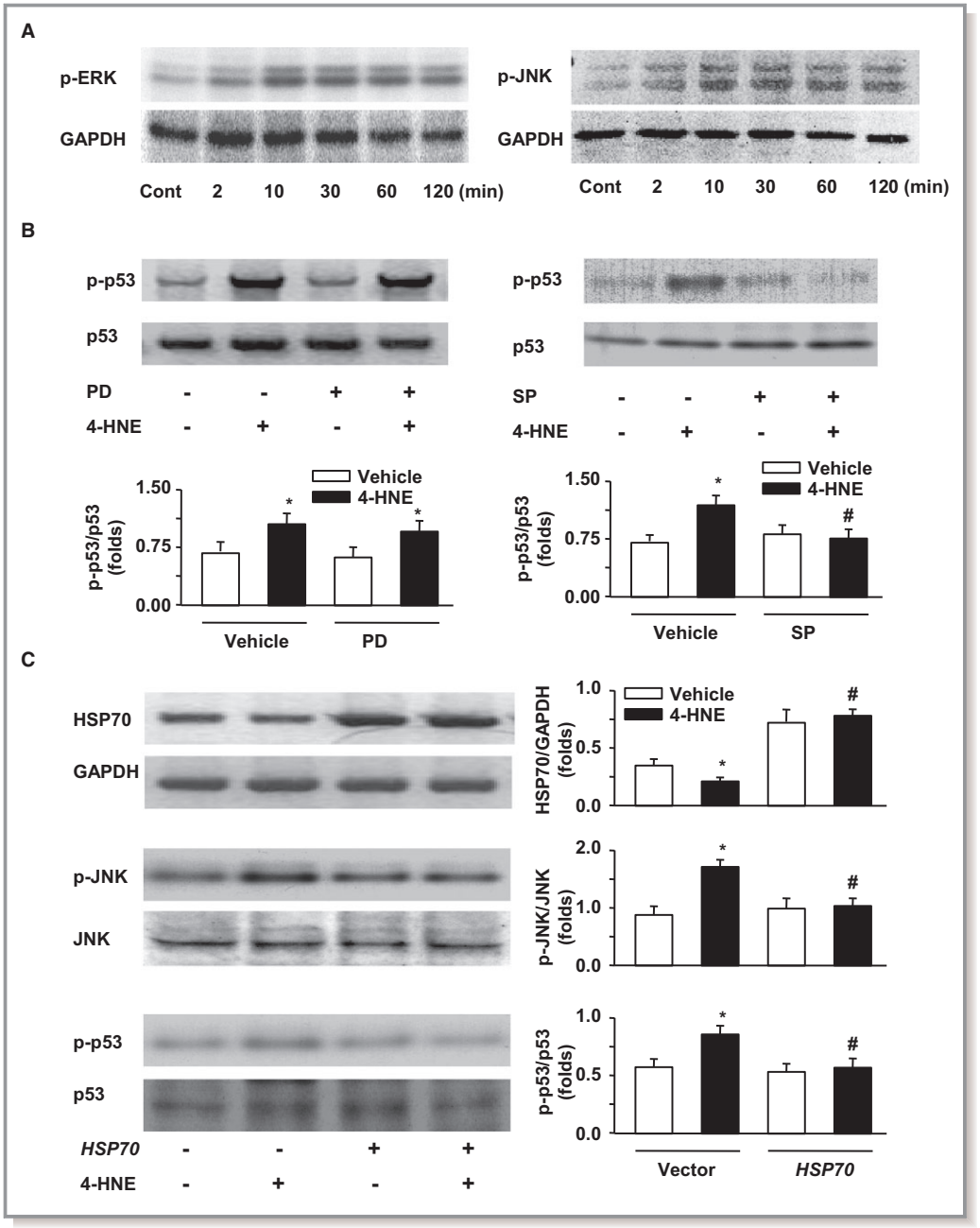

Figure 12. Involvement of HSP70 and JNK in 4-HNE–induced p53 phosphorylation. A, Western blot analysis for 4-HNE–induced time-dependent ERK or JNK phosphorylation in cultured cardiomyocytes. Cultured cardiomyocytes were stimulated with 4-HNE for the indicated times. Phosphorylations of ERKs and JNK were detected by respective antibodies. GAPDH was used as a loading control. Representative photographs are shown. B, Western blot analysis for p-p53 in cultured cardiomyocytes with or without PD or SP pretreatment. Cultured cardiomyocytes were pretreatment with PD or SP for 30 minutes and then stimulated with 4-HNE for 2 hours. p53 was used as an internal control. Representative photographs are shown. The p-p53 was quantified as folds of p53. Data are shown as mean±SE from 9 samples. **P*<0.05 vs respective vehicle. #*P*<0.05 vs respective 4-HNE with vehicle. (C) Effects of HSP70 on 4-HNE–induced JNK and p53 phosphorylation. Cultured cardiomyocytes were transfected by an adenovirus-vector encoding HSP70 (*HSP70* +) or empty vector (*HSP70* −) for 24 hours, and then stimulated with 4-HNE (+) for 30 minutes (for p-JNK) or 2 hours (for p-p53) or with vehicle (−). GAPDH, JNK, and p53 were used as respective internal controls. Representative photographs are shown. HSP70, p-p53, and p-JNK were quantified as folds of GAPDH, JNK, and p53, respectively. Data are shown as mean±SE from 9 samples. **P*<0.05 vs respective vehicle. #*P*<0.05 vs respective 4-HNE with vector. − indicates negative; +, positive; 4-HNE, 4-hydroxy-2-nonenal; Cont, control; p, phosphorylated; PD, PD98059; SP, SP600125; Vector, empty vector.

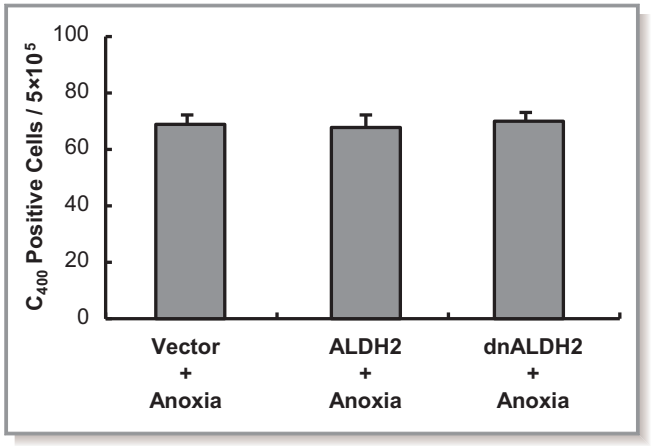

Figure 13. Effects of ALDH2 on reactive oxygen species generation in cardiomyocytes. Cultured cardiomyocytes were transfected with empty vector, *ALDH2*, and *dnALDH2* for 24 hours and exposed to anoxia for 2 hours. The cells were treated with DCFH-DA and then analyzed by a flow cytometry using excitation and emission filters of 488 and 525 nm. The increases in fluorescence emission of DCF, a derivative of DCFH-DA, reflect the enhanced cellular oxidative stress. There were no differences among 3 groups. ALDH2 indicates aldehyde dehydrogenase 2; DCF, dichlorofluorescein; DCFH-DA, 2′,7′-dichlorodihydrofluorescein diacetate. dnALDH2, dominant negative forms of *ALDH2*.

We next examined whether 4-HNE itself affected p53 expression and phosphorylation. Perfusion of the isolated heart with 4-HNE for 2 hours induced a significant increase in the phosphorylation level of p53 (Figure 11F). Treatment with Pft, a specific p53 inhibitor, significantly inhibited 4-HNE–induced apoptosis in cultured cardiomyocytes (Figure 11G). Furthermore, in vivo administration of *p53* siRNA, which efficiently suppressed the expression of p53 at both mRNA and protein levels (Figure 3A and 3B), significantly attenuated 4-HNE–induced cardiomyocyte apoptosis (Figure 11H). These results suggest that 4-HNE accumulation, a consequence of ALDH2 downregulation, could induce cardiomyocyte apoptosis through a p53-dependent pathway.

Involvement of HSP70 and JNK in 4-HNE-Induced Phosphorylation of p53

It was reported that the 2 members of MAP kinase family, the ERKs and JNK, were actively involved in the activation of p53 and apoptosis in L929 cells.[33] We explored their roles in 4-HNE stimulated cardiomyocytes. 4-HNE significantly activated both ERKs and JNK in cardiomyocytes in a time-dependent manner (Figure 12A), and pretreatment with JNK inhibitor SP600125, but not ERKs inhibitor PD98059, significantly attenuated 4-HNE–induced phosphorylation of p53 (Figure 12B), suggesting that JNK but not ERK might serve as a mediator for 4-HNE–induced p53 phosphorylation and apoptosis in cultured cardiomyocytes.

We previously reported that HSP70 suppressed the activation of JNK under hypoxia conditions in cardiomyocytes,[26] so the role of HSP70 in 4-HNE–induced phosphorylation of JNK and p53 was investigated. Our results showed that HSP70 (Figure 12C), but not HSF1 (data not shown), was

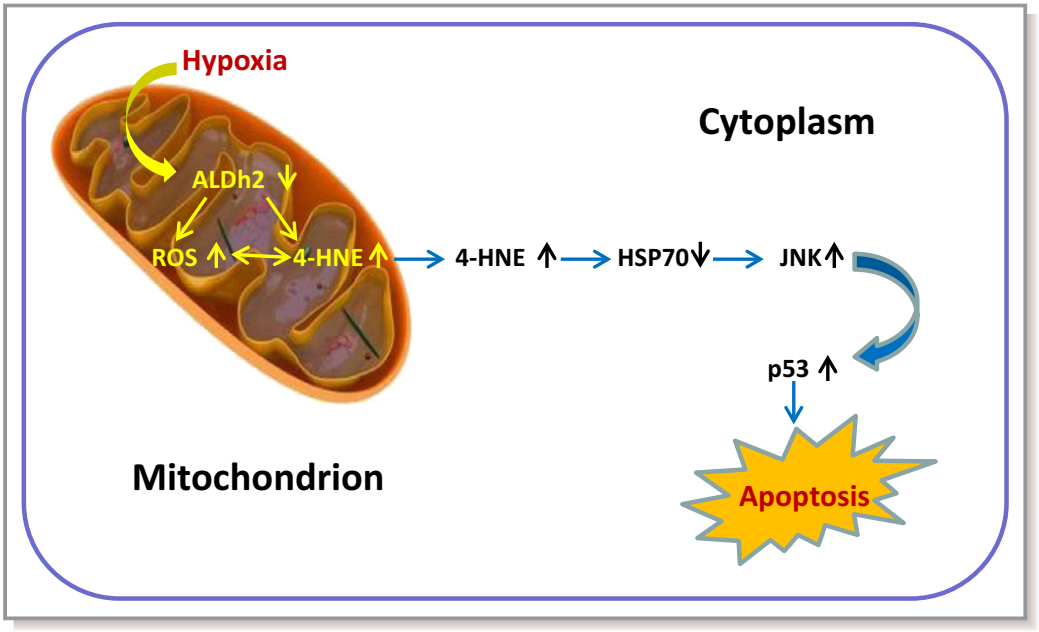

Figure 14. Proposed mechanism underlying the effects of ALDH2 on heart failure and the promising therapeutic targets. 4-HNE indicates 4-hydroxy-2-nonenal; ALDH2, aldehyde dehydrogenase 2; ROS, Reactive Oxygen Species.

significantly downregulated in 4-HNE–treated cardiomyocytes, and transfection of *HSP70* into cardiomyocytes abrogated 4-HNE–induced phosphorylation of JNK and p53 (Figure 12C). These results suggest that 4-HNE could downregulate HSP70 independently of HSF1, leading to the activation of JNK and p53 and apoptosis of cardiomyocytes.

Discussion

In the present study, downregulation of ALDH2 was identified during the development of HF after MI. Loss and gain of function of ALDH2 respectively aggravated and attenuated hypoxia-induced cardiomyocyte apoptosis and HF after MI. ALDH2 detoxifies 4-HNE, a mediator of programmed cell death events, by transmitting a mitochondrial ALDH2 signal to elicit a cytosolic response through the JNK/p53 pathway.

It has been shown that activation of mitochondrial ALDH2 by a small-molecule activator, Alda-1, reduces ischemic damage after MI in rats.[17] In this paper, we provide mechanistic insights into the homeostatic function of ALDH2 in the heart under ischemic conditions. Our present study revealed that the number of apoptotic cardiomyocytes was increased in the *ALDH2*-KO mice but was decreased by overexpression of *ALDH2* in the infarcted heart. The experiments using cultured cardiomyocytes also showed that *ALDH2*-transfected cardiomyocytes were more resistant to anoxia-induced apoptosis, whereas *dnALDH2*-transfected cardiomyocytes were more susceptible compared with mock-transfected cells. These results suggest that downregulation of ALDH2 after MI induces apoptosis of cardiomyocytes and contributes to the development of HF.

Upregulation of mitochondrial ALDH2 reduces cardiac injuries after MI through decrease of 4-HNE,[17] a finding that is consistent with our results that downregulation of ALDH2 after MI induces accumulation of 4-HNE, leading to increases in cardiomyocyte apoptosis; however, its precise mechanism, especially how 4-HNE induces cardiomyocyte death, is still unclear. A major ROS is mitochondrially derived superoxide anion radical, which attacks polyunsaturated fatty acids, leading to membrane lipid peroxidation, thereby generating reactive aldehydes including 4-HNE.[30] A previous study reported that upregulation of ALDH2 prevents apoptosis of human umbilical vein endothelial cells by decreasing ROS generation.[34] Another study showed that ALDH2 protects neuronal cells against oxidative stress by detoxifying 4-HNE rather than attenuating ROS generation.[28] In the present study, ROS was not involved in ALDH2-mediated protection of the heart during the development of HF after MI because transfection of either ALDH2 or its dominant negative mutants did not change ROS production in hypoxic cardiomyocytes (Figure 13). These results suggest that ROS is not involved in the downstream pathways of ALDH2 effects. However, transfection of ALDH2 or dnALDH2 respectively suppressed or enhanced anoxia-induced increases in 4-HNE in cardiomyocytes, indicating that ALDH2 protects cardiomyocytes, at least partially, through reducing 4-HNE.

4-HNE, a diffusible product of membrane lipid peroxidation, has been suggested as a key mediator of oxidative stress–induced cell death.[31] 4-HNE has been reported to induce upregulation and phosphorylation of p53 in retinal pigment epithelial cells.[31] Our in vitro and ex vivo experiments clearly demonstrated that 4-HNE induced functional activation of p53 and enhanced cardiomyocyte apoptosis. Either inhibition of p53 by inhibitor or knockdown of p53 by siRNA attenuated 4-HNE-induced cardiomyocyte apoptosis. These data collectively demonstrate that ALDH2-downregulation–dependent 4-HNE production after MI induces cardiomyocyte apoptosis, at least in part, through activation of the p53 pathway.

It has been unclear how 4-HNE induces functional activation of p53. In the present study, 4-HNE induced phosphorylation of JNK, and JNK inhibitor significantly suppressed 4-HNE–induced phosphorylation of p53. Although 4-HNE induced increases in the phosphorylation of ERKs, inhibition of ERKs could not suppress 4-HNE–induced phosphorylation of p53. In addition, 4-HNE could not affect the phosphorylation levels of the p38MAP kinase. These results suggest that JNK, but not ERKs or p38MAP kinase, is critical to the ALDH2/4-HNE–induced functional activation of p53. Furthermore, 4-HNE downregulated HSP70, and overexpression of HSP70 abrogated 4-HNE–induced phosphorylation of JNK and p53. Because we previously reported that HSP70 may bind to and inhibit phosphorylation of JNK,[26] our results strongly suggest that 4-HNE induced functional activation of p53, at least partially, through dowregulation of HSP70 and activation of JNK. The 4-HNE/HSP70/JNK-p53 pathway may act as an essential ALDH2 cytosolic partner, jointly participating in a coordinated multiorganelle event in the failing myocardium.

It was reported recently that overexpression of ALDH2 antagonizes chronic development of alcoholic cardiomyopathy through phosphorylation of apoptosis signal-regulating kinase 1, glycogen synthase kinase-3β, GATA binding protein 4, and cAMP response-element binding protein.[18] The data from same group also indicated that ALDH2 overexpression antagonizes chronic alcohol intake–induced cardiac insulin insensitivity and contractile defect via improvement of insulin signaling at the levels of insulin receptor, insulin receptor substrate, protein kinase B/Akt, Foxo3a, and JNK.[34] Quite recently, proinflammatory cytokine macrophage migration inhibitory factor has been shown to regulate mammalian target of rapamycin signaling to activate autophagy to preserve cardiac geometry and protect against cardiac injuries.[36] Whether these proteins take part in the mecha-

nistic event in our present post-MI setting needs to be addressed in a future study.

In summary, our results suggest that ischemic injury could result in downregulation of mitochondrial ALDH2 in mice hearts after MI, leading to 4-HNE accumulation. The increased 4-HNE transmits the mitochondrial signal to cytosol, enhancing cardiomyocyte apoptosis through downregulation of HSP70 and activation of JNK and p53, and thereby promotes the development of HF (Figure 14). Enhancing myocardial ALDH2 expression or activity might emerge as a promising therapeutic strategy for HF.

Acknowledgments

We thank Dr Shigeo Ohta at Nippon Medical School, Tokyo, Japan, for kindly providing the *ALDH2* plasmids. We thank Jianguo Jia and Bingyu Li at Zhongshan Hospital and Guoping Zhang at Institute of Biomedical Science, Fudan University, Shanghai, China, for technical assistance.

Sources of Funding

Key Program of National Natural Science Foundation of China (30930043), National Natural Science Foundation of China (30971250), National Basic Research Program of China (2007CB512003), China Doctoral Foundation (20110071110051), the Science and Technology Commission of Shanghai Municipality (11JC1402400).

Disclosures

None.

References

1. Cleland JG, Khand A, Clark A. The heart failure epidemic: exactly how big is it. *Eur Heart J*. 2001;22:623–626.
2. Kociol RD. Most important papers in pathophysiology and genetics. *Circ Heart Fail*. 2012;5:32–49.
3. Goffart S, von Kleist-Retzow JC, Wiesner RJ. Regulation of mitochondrial proliferation in the heart: power-plant failure contributes to cardiac failure in hypertrophy. *Cardiovasc Res*. 2004;64:198–207.
4. Huss JM, Kelly DP. Mitochondrial energy metabolism in heart failure: a question of balance. *J Clin Invest*. 2005;115:547–555.
5. Giordano FJ. Oxygen, oxidative stress, hypoxia, and heart failure. *J Clin Invest*. 2005;115:500–508.
6. Gong G, Liu J, Liang P, Guo T, Hu Q, Ochiai K, Hou MX, Ye Y, Wu XY, Mansoor A, From AHL, Ugurbil K, Bache RJ, Zhang JY. Oxidative capacity in failing hearts. *Am J Physiol Heart Circ Physiol*. 2003; 285:H541–H548.
7. Grieve DJ, Shah AM. Oxidative stress in heart failure. More than just damage. *Eur Heart J*. 2003;4:2161–2163.
8. Kocher AA, Schuster MD, Szabolcs MJ, Takuma S, Burkhoff D, Wang J, Homma S, Edwards NM, Itescu S. Neovascularization of ischemic myocardium by human bone-marrow-derived angioblasts prevents cardiomyocyte apoptosis, reduces remodeling and improves cardiac function. *Nat Med*. 2001;7:430–436.
9. Crow MT, Mani K, Nam YJ, Kitsis RN. The mitochondrial death pathway and cardiac myocyte apoptosis. *Circ Res*. 2004;95:957–970.
10. Regula KM, Kirshenbaum LA. Apoptosis of ventricular myocytes: a means to an end. *J Mol Cell Cardiol*. 2005;38:3–13.
11. Wencker D, Chandra M, Nguyen K, Miao W, Garantziotis S, Factor SM, Shirani J, Armstrong RC, Kitsis RN. A mechanistic role for cardiac myocyte apoptosis in heart failure. *J Clin Invest*. 2003;111:1497–1504.
12. Chen Z, Zhang J, Stamler JS. Identification of the enzymatic mechanism of nitroglycerin bioactivation. *Proc Natl Acad Sci USA*. 2003;99:8306–8311.
13. Mackenzie IS, Maki-Petaja KM, McEniery CM, Bao YP, Wallace SM, Cheriyan J, Monteith S, Brown MJ, Wilkinson IB. Aldehyde dehydrogenase 2 plays a role in the bioactivation of nitroglycerin in humans. *Arterioscler Thromb Vasc Biol*. 2005;25:1891–1895.
14. Chen Z, Foster MW, Zhang J, Mao L, Rockman HA, Kawamoto T, Kitagawa K, Nakayama KI, Hess DT, Stamler JS. An essential role for mitochondrial aldehyde dehydrogenase in nitroglycerin bioactivation. *Proc Natl Acad Sci USA*. 2005;102:12159–12164.
15. Li Y, Zhang D, Jin W, Shao C, Yan P, Xu C, Sheng H, Liu Y, Yu J, Xie Y, Zhao Y, Lu D, Nebert DW, Harrison DC, Huang W, Jin L. Mitochondrial aldehyde dehydrogenase-2 (ALDH2) Glu504Lys polymorphism contributes to the variation in efficacy of sublingual nitroglycerin. *J Clin Invest*. 2006;116:506–511.
16. Oyama T, Isse T, Ogawa M, Muto M, Uchiyama I, Kawamoto T. Susceptibility to inhalation toxicity of acetaldehyde in Aldh2 knockout mice. *Front Biosci*. 2007;12:1927–1934.
17. Chen CH, Budas GR, Churchill EN, Disatnik MH, Hurley TD, Mochly-Rosen D. Activation of aldehyde dehydrogenase-2 reduces ischemic damage to the heart. *Science*. 2008;321:1493–1495.
18. Doser TA, Turdi S, Thomas DP, Epstein PN, Li SY, Ren J. Transgenic overexpression of aldehyde dehydrogenase-2 rescues chronic alcohol intake-induced myocardial hypertrophy and contractile dysfunction. *Circulation*. 2009;119:1941–1949.
19. Fan F, Sun A, Zhao H, Liu X, Zhang W, Jin X, Wang C, Ma X, Shen C, Zou Y, Hu K, Ge J. MicroRNA-34a promotes cardiomyocyte apoptosis post myocardial infarction through down-regulating aldehyde dehydrogenase 2. *Curr Pharm Des*. 2013;19:4865–4873.
20. Isse T, Oyama T, Matsuno K, Ogawa M, Narai-Suzuki R, Yamaguchi T, Murakami T, Kinaga T, Uchiyama I, Kawamoto T. Paired acute inhalation test reveals that acetaldehyde toxicity is higher in aldehyde dehydrogenase 2 knockout mice than in wild-type mice. *J Toxicol Sci*. 2005;30:329–337.
21. Sano M, Minamino T, Toko H, Miyauchi H, Orimo M, Qin Y, Akazawa H, Tateno K, Kayama Y, Harada M, Shimizu I, Asahara T, Hamada H, Tomita S, Molkentin JD, Zou Y, Komuro I. p53-induced inhibition of Hif-1 causes cardiac dysfunction during pressure overload. *Nature*. 2007;446:444–448.
22. Zou Y, Li J, Ma H, Jiang H, Yuan J, Gong H, Liang Y, Guan A, Wu J, Li L, Zhou N, Niu Y, Sun A, Nakai A, Wang P, Takano H, Komuro I, Ge J. Heat shock transcription factor 1 protects heart after pressure overload through promoting myocardial angiogenesis in male mice. *J Mol Cell Cardiol*. 2011;51:821–829.
23. Hilfiker-Kleiner D, Hilfiker A, Kaminski K, Schaefer A, Park JK, Michel K, Quint A, Yaniv M, Weitzman JB, Drexler H. Lack of JunD promotes pressure overload-induced apoptosis, hypertrophic growth, and angiogenesis in the heart. *Circulation*. 2005;112:1470–1477.
24. Yin C, Xi L, Wang X, Eapen M, Kukreja RC. Silencing heat shock factor 1 by small interfering RNA abrogates heat shock-induced cardioprotection against ischemia-reperfusion injury in mice. *J Mol Cell Cardiol*. 2005;39:681–689.
25. National Research Council (US) Institute for Laboratory Animal Research. Guide for the Care and Use of Laboratory Animals. Washington (DC): National Academies Press (US); 1996.
26. Harada M, Qin Y, Takano H, Minamino T, Zou Y, Toko H, Ohtsuka M, Matsuura K, Sano M, Nishi J, Iwanaga K, Akazawa H, Kunieda T, Zhu W, Hasegawa H, Kunisada K, Nagai T, Nakaya H, Yamauchi-Takihara K, Komuro I. G-CSF prevents cardiac remodeling after myocardial infarction by activating the Jak-Stat pathway in cardiomyocytes. *Nat Med*. 2005;11:305–311.
27. Zou Y, Zhu W, Sakamoto M, Qin Y, Akazawa H, Toko H, Mizukami M, Takeda N, Minamino T, Takano H, Nagai T, Nakai A, Komuro I. Heat shock transcription factor 1 protects cardiomyocytes from ischemia/reperfusion injury. *Circulation*. 2003;108:3024–3030.
28. Ohsawa I, Nishimaki K, Yasuda C, Kamino K, Ohta S. Deficiency in a mitochondrial aldehyde dehydrogenase increases vulnerability to oxidative stress in PC12 cells. *J Neurochem*. 2003;84:1110–1117.
29. Fujimoto M, Takaki E, Hayashi T, Kitaura Y, Tanaka Y, Inouye S, Nakai A. Active HSF1 significantly suppresses polyglutamine aggregate formation in cellular and mouse models. *J Biol Chem*. 2005;280:34908–34916.
30. Bhatnagar A. Electrophysiological effects of 4-hydroxynonenal, an aldehydic product of lipid peroxidation, on isolated rat ventricular myocytes. *Circ Res*. 1995;76:293–304.

31. Sharma A, Sharma R, Chaudhary P, Vatsyayan R, Pearce V, Jeyabal PVS, Zimniak P, Awasthi S, Awasthi YC. 4-Hydroxynonenal induces p53-mediated apoptosis in retinal pigment epithelial cells. *Arch Biochem Biophys*. 2008;480:85–94.
32. Moorjani N, Catarino P, Trabzuni D, Saleh S, Mooji A, Dzimiri N, Al-Mohanna F, Westaby S, Ahmad M. Upregulation of Bcl-2 proteins during the transition to pressure overload-induced heart failure. *Int J Cardiol*. 2007; 116:27–33.
33. Cheng Y, Qiu F, Tashiro S, Onodera S, Ikejima T. ERK and JNK mediate TNFalhpa-induced p53 activation in apoptotic and autophagic L929 cell death. *Biochem Biophys Res Commun*. 2008;376:483–488.
34. Li SY, Gomelsky M, Duan JH, Zhang ZJ, Gomelsky L, Zhang XC, Epstein PN, Ren J. Overexpression of aldehyde dehydrogenase-2 (ALDH2) transgene prevents acetaldehyde-induced cell injury in human umbilical vein endothelial cells: role of ERK and p38 mitogen-activated protein kinase. *J Biol Chem*. 2004;279:11244–11252.
35. Li SY, Gilbert SA, Li Q, Ren J. Aldehyde dehydrogenase-2 (ALDH2) ameliorates chronic alcohol ingestion-induced myocardial insulin resistance and endoplasmic reticulum stress. *J Mol Cell Cardiol*. 2009;47:247–255.
36. Xu X, Hua Y, Nair S, Bucala R, Ren J. Macrophage migration inhibitory factor deletion exacerbates pressure overload-induced cardiac hypertrophy through mitigating autophagy. *Hypertension*. 2014;63:490–499.